Université Abdou Moumouni - Niamey

Doctoral Research Program - Climate Change and Energy (DRP-CCE)

Republic of NIGER

INTERNATIONAL MASTER PROGRAM

IN RENEWABLE ENERGY AND GREEN HYDROGEN

SPECIALITY: PHOTOVOLTAICS FOR GREEN HYDROGEN TECHNOLOGY

MASTER THESIS

Topic:

CHARACTERIZATION OF DIRECT LIGHT SOAKING EFFECT ON TRANSPARENT PASSIVATING CONTACT SOLAR CELLS

Presented by: **Penda FALL**

Date: 28th September 2023

Defense Committee Members

Chairman : Pr. Makinta Boukar, Abdou Moumouni University - Niger

Examiner : Dr. Souley Kallo Moutari, Abdou Moumouni University - Niger

Main supervisors : Dr. Kaining Ding, Forschungszentrum Jülich - Germany

Pr. Dr. Uwe Rau, Forschungszentrum Jülich - Germany

Local supervisor : Ass. Prof. Halidou Ibrahim, Abdou Moumouni University - Niger

Academic year 2022-2023

Characterization of Direct Light Soaking Effect on Transparent Passivating Contact Solar Cells

Presented by
Penda Fall

Master's Thesis in Photovoltaics for Green-H_2
submitted to the

Faculty of Sciences and Techniques
Department of Physics of Abdou Moumouni University-Niger
in September 2023

This thesis was written at the Research Centre Jülich, Institute for Energy and Climate Research, Photovoltaics (IEK-5)

ACKNOWLEDGEMENTS

I hereby thank all people and organizations that supported me during my Master's program:

The German Federal Ministry of Education and Research (BMBF) and especially Pr. Christoph Rövekamp, Head of "Energy and Hydrogen Technologies" division 722 for the full scholarship.

The West African Science Service Centre on Climate Change and Adapted Land Use (WASCAL) for organizing the program.

The Université Abdou Moumouni of Niamey (UAM) from which I will be graduating.

The Director of IEK-5/Forschungszentrum Jülich Prof. Dr. Uwe Rau, for welcoming me to his institute and for the knowledge he shared during the "Fundamentals of Photovoltaics" and "Characterization and Simulation of Solar Cells" courses.

The Director of WASCAL DRP-CCE Niger Prof. Rabani Adamou for his pieces of advice and knowledge shared during the program.
The IMPEGH coordinator of WASCAL DRP-CCE Niger Dr. Abdoulkadri Ayouba Mahamane and the whole staff in Niger, for monitoring the courses, exams, and activities.

My supervisors, Dr. Kaining Ding and Ass. Prof. Halidou Ibrahim for their supervision and constructive feedback.
Binbin Xu for his commitment and availability which motivated me to strive for excellence. His assistance has indeed made this endeavor possible.

The jury members for their diligent evaluation which helps in validating the credibility of this work: Pr. Makinta Boubar, President of the jury; Dr. Souley Kallo Moutari, Examiner; Pr. Dr. Uwe Rau; Ass. Pr. Halidou Ibrahim and Dr. Kaining Ding.

The Advanced SHJ technology team at IEK-5 for their feedback during the weekly meetings which guided me in the achievement of meaningful results. Volker Lauterbach for his unwavering support with the Light Soaking and the LOANA solar cell systems.

My family and Arouna Khalil Fanny for their moral support, prayers, and confidence. May all those not mentioned, who supported me in one way or another, find here the expression of my deepest gratitude.

ABSTRACT

The optimization of a transparent, passivating, and conductive contact approach for the front side of silicon heterojunction solar cells has been widely studied due to the observed parasitic absorption losses in the amorphous silicon layers and the passivation losses during Indium Tin Oxide sputtering. To enable high-efficiency crystalline silicon solar cells based on the combined front transparent passivating contact surface and rear silicon heterojunction structure, the present study focuses on curing the sputter damage by the application of light soaking without pre-annealing treatment. The investigation of different light soaking conditions defines the heat-assisted light soaking performed at 175 ℃ during 360s as a suitable operating condition to characterize the process on transparent passivating contact solar cells. The combination of heat and light during the curing process was found to be an inseparable effect in order to achieve better performance. A significant reduction in the open-circuit voltage loss is observed after direct light soaking curing, resulting in a passivation recovery. The measurement of the photovoltaic parameters shows an interesting overall power conversion efficiency of 23.4% achieved for an open-circuit voltage of 736 mV, a fill factor of 80%, a short-circuit current density of 39.75 mA/cm^2, and 1.146 Ω cm^2 as a contribution of series resistance. The study demonstrates the potential of direct light soaking to improve the transparent passivating and conductive contact solar cells and contributes to a better understanding of the internal mechanisms involved.

Keywords: silicon heterojunction; transparent passivating and conductive contact; sputter damage; open-circuit voltage loss; light soaking.

RÉSUMÉ

L'optimisation du contact transparent, passivant et conducteur réalisé sur la face-avant des cellules solaires à hétérojonction en silicium a été largement étudiée en raison des pertes d'absorption parasites observées dans les couches de silicium amorphe et des pertes de passivation pendant la pulvérisation d'oxyde d'étain et d'indium. Afin d'obtenir des cellules solaires au silicium cristallin à haut rendement basées sur la structure combinée du contact transparent, passivant et conducteur en face-avant avec la structure hétérojonction à silicium en face-arrière, la présente étude se concentre sur le traitement des pertes causées par la pulvérisation en procédant par imbibition de la lumière ou photo-trempage sans pré-traitement thermique. L'étude de différentes conditions d'imbibition de lumière définit le photo-trempage assisté par la chaleur effectué à 175°C pendant 360s comme la condition de traitement appropriée pour caractériser le processus sur les cellules solaires considérées. La combinaison de la chaleur et de la lumière durant le processus s'est avérée être un effet inséparable pour obtenir une meilleure performance. Une réduction significative des pertes en tension de circuit ouvert est observée après le traitement par imbibition de la lumière, entraînant un recouvrement de la passivation. La mesure des paramètres photovoltaïques montre un intéressant rendement global de 23,4 % pour une tension en circuit ouvert de 736 mV, un facteur de forme de 80 %, une densité de courant de court-circuit de 39,75 mA/cm^2 et 1,146 Ω cm^2 comme contribution à la résistance en série. L'étude démontre le potentiel du photo-trempage pour améliorer le rendement des cellules solaires à contact transparent, passivant et conducteur et contribue à une meilleure compréhension des mécanismes internes impliqués.

Mots-clés : Hétérojonction de silicium ; contact transparent passivant et conducteur ; pertes de pulvérisation ; pertes en tension de circuit ouvert ; imbibition de la lumière ou photo-trempage.

ACRONYMS AND ABBREVIATIONS

ORGANIZATIONS AND INSTITUTIONS

BMBF : Bundesministerium für Bildung und Forschung

FZJ : Forschungszentrum Jülich

IEK-5 : Institut für Energie- und Klimaforschung Photovoltaik

IMPEGH : International Master Program in Energy and Green Hydrogen

UAM : Université Abdou Moumouni

WASCAL : West African Science Service Center on Climate Change and Adapted Land Use

SOLAR CELLS AND SAMPLES' LAYERS

a-Si : Amorphous Silicon

a-Si:H(i) : Intrinsic hydrogenated amorphous silicon

a-Si:H(n) : n-doped hydrogenated amorphous silicon

a-Si:H(p) : p-doped hydrogenated amorphous silicon

c-Si(n) : n-doped crystalline silicon

ITO : Indium Tin Oxide

nc-SiC:H(n) cond. : n-doped hydrogenated nanocrystalline silicon carbide conductive layer

nc-SiC:H(n) pass. : n-doped hydrogenated nanocrystalline silicon carbide passivating layer

SHJ : Silicon Heterojunction

SiO_x : Silicon tunnel oxide

TPC : Transparent Passivating and Conductive contact

PROCESSING TECHNIQUES AND CHARACTERIZATION METHODS

HWCVD : Hot Wire Chemical Vapor Deposition

LiSo : Light Soaking

PECVD : Plasma Enhanced Chemical Vapor Deposition

EL : Electroluminescence

FTIR : Fourier Transform Infrared spectroscopy

PL : Photoluminescence

QSSPC : Quasi-steady state photoconductance

TLM : Transmission Line Method / Transfer Length Method

LIST OF TABLES

LIST OF FIGURES

CONTENTS

INTRODUCTION

1. Background

Reforming the global energy system to reduce the greenhouse gas emissions is one of the most important approaches in today's energy transition. In West Africa for example, the impacts of climate change on nature, humans and life have increased significantly in recent years and this is expected to rise, while the continent is the lowest contributor to greenhouse gas emissions globally[1]. Since the limitation of global warming is crucial in preventing the worst impacts of climate change, the electricity generation capacity is gradually moving towards renewables through more common sources such as wind, solar, hydroelectricity and biomass. As of 2021, almost one quarter of the electricity produced worldwide comes from renewables[2] with a share of 4.52 % for solar energy[3]. The total cumulative solar capacity installed worldwide was 940 GW[4], showing that the market of solar photovoltaic technology and renewables in general is in full expansion as a response to the call for net zero emissions. This energy transition, which sees the use of renewable energies as an alternative to fossil fuels for power generation, heating, and cooling, requires stable, highly efficient technologies to improve access to clean electricity and clean energy.

The development of the Photovoltaic (PV) technology offers many benefits in comparison to other clean or traditional technologies. Besides being environmentally friendly, the technology produces no noise, no toxic gases and the electricity is produced through a zero-emission process. The conversion of solar energy into electricity by means of the photovoltaic technology is possible via the photovoltaic effect. In manufacturing the photovoltaic solar cells, several materials are used, from the crystalline silicon-based materials to the thin-film solar cells and the dye-sensitized solar cells. In the case of the crystalline silicon-based solar cells (c-Si), prior researches have introduced the silicon heterojunction (SHJ) solar cells as a favorable option, offering advantages such as cost-reduction, high efficiency, better temperature coefficient and high bifacial ratio in comparison to other crystalline silicon-based solar cells.

The mainstream SHJ structure is composed of a c-Si wafer sandwiched between the n-type doped/intrinsic hydrogenated amorphous silicon layers (a-Si:H) at the front side and the intrinsic/p-type doped a-Si:H layers at the rear side with a layer of Indium Tin Oxide (ITO)

deposited on both front and back sides. For the fabrication of the solar cell based on the SHJ architecture, high efficiencies are achieved with lower energy costs [5]. The potential of SHJ and other polycrystalline silicon (poly-Si) with carrier-selective passivating contacts has been widely demonstrated as a result of the development in the structure and design with a recorded efficiency exceeding 26 % [6]. An important demarcation point in the diversification of manufacturing high-efficiency SHJ solar cells is the application at the front side, of a passivating contact approach. This surface reduces the recombination losses at the contacts and helps to approach the theoretical and practical limits of the cell's efficiency [7].

Due to the significant optical absorption losses in the top a-Si:H layers and the need for high doping efficiency with an elimination of the Schottky barrier, the transparent passivating and conductive contact (TPC) concept at the front side of silicon heterojunction solar cells has been developed and is at the heart of this thesis. As demonstrated by K. Ding et *al.* [8], the excellent surface passivation for c-Si wafers is obtained by combining the SiO_2 layer with the highly-doped hydrogenated microcrystalline silicon-carbide (µc-SiC:H) layer sometimes refers to as hydrogenated nanocrystalline silicon-carbide (nc-SiC:H). Therefore, the TPC concept investigated in this study consists of a double-layer n-type doped nc-SiC:H (a conductive layer and a passivating layer) in contact with the silicon oxide (SiO_x) layer. At the interface between SiO_x and c-Si layer, defects are passivated, for example by the presence of hydrogen from the upper layers or oxygen from SiO_x. The aim of this transparent passivating surface is to enable a good front side contact of the c-Si with a high transparency in AM1.5G, a good passivation at the surface and a good conductivity [9]. Compared to the SHJ concept, the TPC approach offers a better temperature stability [7].

2. Research problem statement

The review of recent studies has given rise to a particular concern: The passivation of TPC solar cells is degraded during ITO deposition by sputtering, which results in a decrease of the open circuit voltage (V_{OC}), thus limiting the efficiency of the cell and its spectral response [10]. The difference of V_{OC} was recorded by M. Köhler et *al.* [11] to be up to 32 mV.

In order to cure the sputter damage on TPC solar cells, a first investigation was done using the pure thermal annealing curing process on a hot plate at high temperature. Results show that

the passivation is improved but the V_{OC} loss is still high, thus the process is unable to significantly recover the passivation quality. Through the combination of thermal curing and light curing, a better improvement of the passivation quality was obtained although still inefficient to remarkably cure the sputter damage. Therefore, the light soaking process without pre- and post-annealing treatments has been proposed. This process could, with the synergistic effect of heat and light, reduce the recombination at the interface and increase the open-circuit voltage V_{OC} and the fill factor *FF* of the material for an improvement of the efficiency. However, some information is currently unclear about the processes and mechanisms involved in the direct soaking process, the parameters and conditions required to recover, potentially fully, the passivation loss and achieve high efficiency.

3. Research questions

From the background of the study and the research problem, some questions still remain:

- Is the direct light soaking a way to completely cure the passivation loss for TPC solar cells?

- Which processing parameters are suitable to characterize the light soaking on TPC solar cell?

- Is the cell performance increased after light soaking?

Thus, the thesis will aim at answering these questions.

4. Research motivation and objectives

The motivation for this study is to solve the issue of passivation loss due to the sputter damage caused by the ITO deposition using the direct light soaking process.

As the performance of the TPC solar cell is intrinsically linked to the good surface passivation, transparency and conductivity, the study also aims at investigating the effect of light soaking on the TPC solar cell performance and find a suitable processing parameter to characterize the process on the cell. This thesis will also contribute to a comprehensive understanding of the underlying mechanisms.

5. Outline of the thesis

For a better understanding of the research topic and findings, the thesis is organized into five (5) parts. The first part is the ongoing introduction which gives an overview of the

photovoltaic technology with a particular interest on silicon-based solar cells. A presentation of the research problem and research questions is also provided as well as the objectives of the study. In chapter 1 of the thesis corresponding to the literature review, the recent technological advancements and actual challenges in the global area of study are discussed. This part also provides more insights on the light soaking process and some fundamentals on TPC and SHJ solar cells. In the second chapter, the materials and characterization methods used are presented and the different steps, from the preparation of the samples to the different measurements for the data collection and data analysis are highlighted. The third chapter is entirely devoted to the results obtained and the discussions. The last part is the conclusion which will give a summary of the work done as well as the perspectives and limitations for future studies.

CHAPTER I: LITERATURE REVIEW

This chapter gives an overview of the mechanisms involved in the study and is divided into three parts: the first section deals with the photovoltaic technology at the cell level and some investigations on the loss mechanisms. In the second part, the fundamentals on SHJ and TPC are presented, and the research problem is developed from the review of the literature. The last part focuses on the light soaking process.

1. State-of-the-art in photovoltaic solar cell

The rapid growth of energy demand and the need to shift to clean energy sources have fostered the development of renewable energy technologies. The power of solar energy in particular is remarkable as the Sun provides about 10,000 times more energy, which is higher than the daily energy needed in the world. Solar energy can be harnessed through the photovoltaic technology and converted into electricity using solar cells through the photovoltaic effect. This effect results in the creation of a voltage or an electric current in a doped semiconductor upon exposure to irradiance[12].

Solar cells are made of absorbers and contacts. The materials used in photovoltaic solar cells are layers of semiconductors (absorbers) most often silicon-based semiconducting p-n junction materials. The semiconductor materials, characterized by a conductivity comprises between an insulator and a conductor, are either intrinsic, n-type doped (excess of electrons), or p-type doped (excess of holes) and the combination of these two regions leads to the creation of a depletion region and subsequently, to the creation of the diffusion and drift currents which give rise to a potential difference within the PN junction.

A schematic representation of the solar cell under illumination is provided in Figure 1. The use of silicon (Si) as a semiconductor in most of the PV solar cells is mainly due to its wide availability as the second abundant material in the earth's crust and its band gap of 1.1 eV closes to the perfect single-junction bandgap. By creating carrier-selective contacts in solar cells, the electrons and holes are collected at the contacts which avoids a recombination of charge carriers.

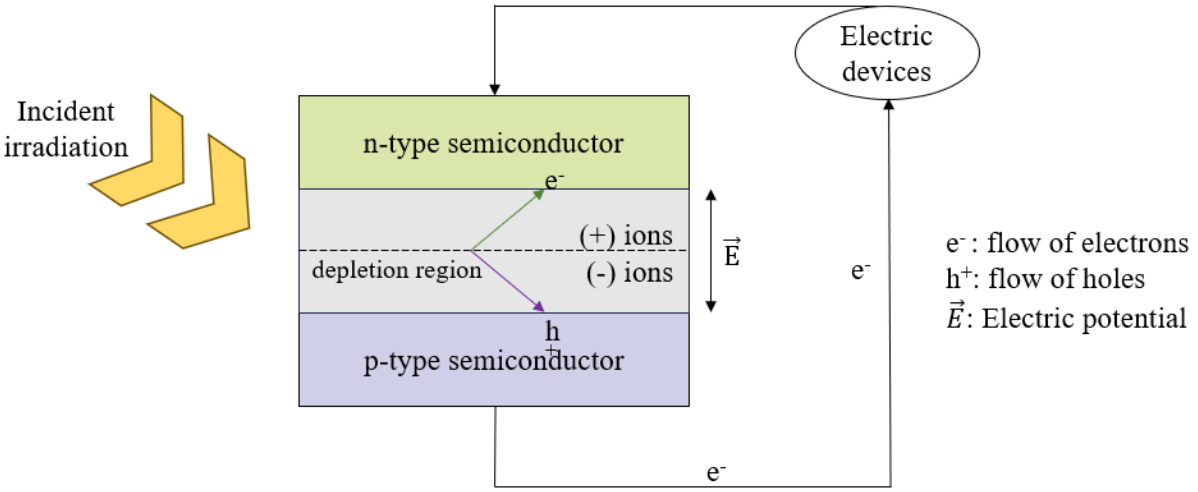

Figure 1: Representation of a solar cell under illumination. Sketched from the idea of [13].

Through theory and experiments, many advancements were made in the PV field. Depending on the properties of the material and the time of their development, three generation of PV technologies exist and were presented in the literature [14][15]. The first generation of PV comprises the solar cells based on the silicon semiconductor materials. In the second generation, the thin-film cells were developed. One important point in this development is the investigation of surface passivation, grid contacts and bifacial cells in 1960's [16]. The third generation is based on novel materials and concepts with low-costs such as perovskite solar cells, dye-sensitized solar cells and organic solar cells. Despite these advancements in the PV materials, achieving high conversion efficiency remains a major concern due to certain loss mechanisms and internal processes that reduce the performance of the solar cell.

To design high efficiency solar cells with good metal contacts, low parasitic absorption, but also with low surface, bulk and junction recombination, researchers mainly worked on the improvement of the absorption of light by the PV materials and the cells structure[17]. One technique developed to increase the absorption of light, is the light trapping which greatly contributes to the improvement of the efficiency[18]. For high quality wafers, some high efficiency cell structures proposed previously are the passivated, emitter and rear cells (PERC), the passivated emitter, rear and totally diffused cells (PERT) and the passivated, emitter, rear locally diffused cells (PERL). Today's markets for solar cells production are dominated by PERC devices [19]. These developments were also possible with the surface passivation and high lifetime boron diffusion processing. A recorded efficiency of 24.7 % were obtained by

PERL cells combined with surface passivation, achieved by oxidation or plasma-enhanced chemical vapor deposition (PECVD silicon nitride deposition), and light trapping process [20]. In the next sub-sections, the main loss mechanisms affecting the solar cell performance are developed and some progress made towards the achievement of higher efficiency are presented.

1.1. Recombination mechanisms

The annihilation of electrons and holes in the non-equilibrium state within the semiconductor material or solar cell is the recombination process. As the generation of electrons and holes occurs in the semiconductor, these charge carriers may also recombine in different regions inside the material and decrease the total number of carriers. The basic principle of generation-recombination of electron-hole pairs is described in figures 2a and 2b.

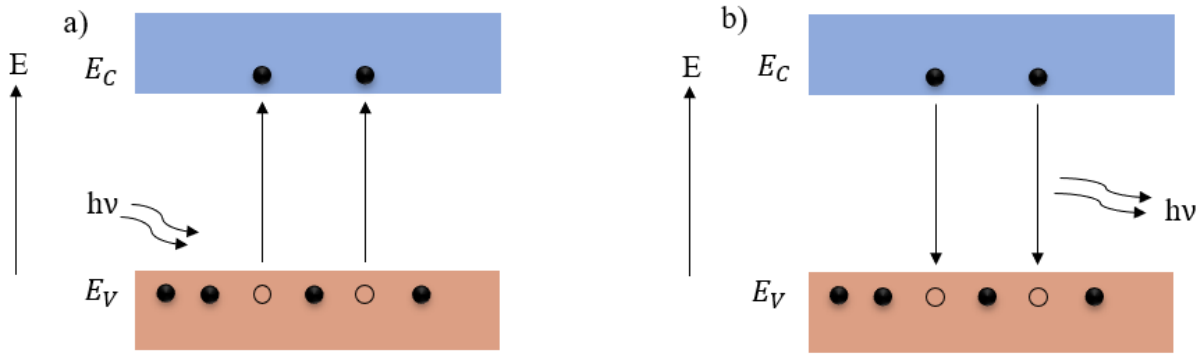

Figure 2: (a) Band-to-band generation (b) Band-to-band recombination

Three recombination mechanisms usually take place in the material: the radiative recombination, the Shockley-Read-Hall recombination and the Auger recombination [21]. As depicted in Figure 3, the radiative recombination (i) allows the emission of a photon from the energy lost by the electron when recombining with the hole in the valence band. In the case of Shockley-Read-Hall recombination (ii), the electron-hole pairs are trapped in the recombination centers and recombine in these forbidden states releasing phonons while the Auger recombination (iii) results in the recombination of an electron and a hole by excitation of a third charge carrier. The recombination rate which is linked to the interface defect density, quantifies the minority carrier recombination and was mentioned by [22] as :

$$R = \frac{\Delta n}{\tau} \tag{1.1}$$

With Δn the injection level or number of excess charge carriers and τ the carrier lifetime.

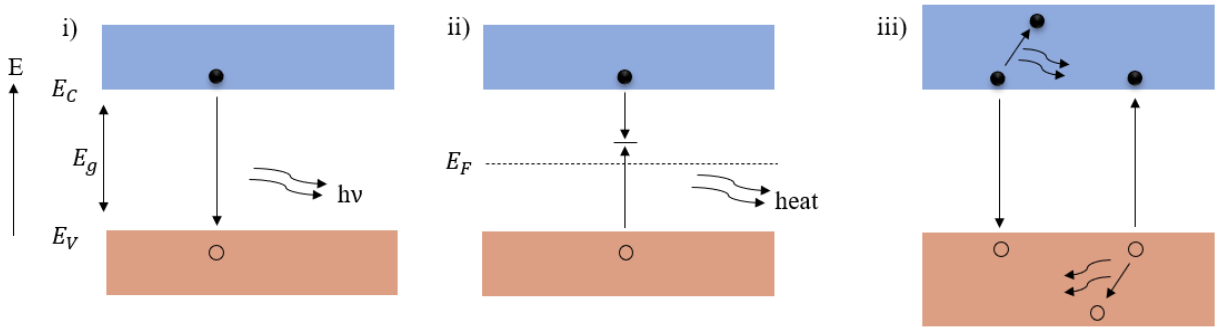

Figure 3: (i) Radiative recombination (ii) SRH recombination (iii) Auger recombination

The bulk lifetime τ_{bulk} is inversely proportional to the inverses of the lifetime for radiative, SRH and Auger processes:

$$\frac{1}{\tau_{\text{bulk}}} = \frac{1}{\tau_{\text{radiative}}} + \frac{1}{\tau_{\text{SRH}}} + \frac{1}{\tau_{\text{Auger}}} \tag{1.2}$$

Another important parameter is the effective carrier lifetime given by Eq (1.3) and linked to bulk lifetime τ_{bulk}, the velocity of the surface recombination S_{eff} and the c-Si thickness D:

$$\frac{1}{\tau_{\text{eff}}} = \frac{1}{\tau_{\text{bulk}}} + \frac{2D}{S_{\text{eff}}} \tag{1.3}$$

Furthermore, low surface recombination velocity (S≈180 cm/s) was achieved for a highly doped µc-SiC:H layer deposited on Si wafer enabling a V_{OC} of 640 mV and 80 % of FF [23].

In solar cell, the lower the recombination, the more efficient is the device. Therefore, limiting the band-gap voltage offset at open-circuit conditions W_{OC} ensures a good quality of the solar cell. It is defined as the difference between the ratio of the band-gap energy E_{g} over the elementary charge q and the open-circuit voltage V_{OC} [24]:

$$W_{\text{OC}} = \frac{E_{\text{g}}}{q} - V_{\text{OC}} \tag{1.4}$$

Auger recombination is one of the most dominant recombination mechanisms in solar cell[25] while SRH recombination originates from impurities and defects in the silicon crystal lattice; however, the reduction of the recombination of photogenerated carriers at the contacts and surface of the c-Si solar cell may enable a high conversion efficiency. Previous

recombination reduction studies mainly focused on the recombination in the volume while the surface and interface recombination directly affect the performance of the cell. Recently, researchers accentuated the investigations on these regions of solar cells. Therefore, the passivating contact approach was developed as an alternative to further tackle the contact recombination losses using some materials such as hydrogenated amorphous silicon a-Si:H [7]. A recombination parameter J_0 also described as the thermal equilibrium recombination current density affecting the current density J produced by the finished solar cell is defined as:

$$J = J_{SC} - J_0 \exp\left(\frac{V}{\frac{kT}{q}} - 1\right) \quad (1.5)$$

With J_{SC} the short-circuit current density, V the voltage, q the charge carrier and kT the thermal energy.

A direct effect of recombination currents in the solar cell is the fill factor losses also related to ohmic series resistance losses. Series resistance R_S are intrinsically linked to the material itself and needs to be reduced for an improved value of the fill factor, a good conductivity and a better power generation capability. The losses due to R_S can be estimated using some methods such as the double-light method (DLM), the $J_{SC} - V_{OC}$ measurement and the calculation at MPP by pseudo fill factor considerations [26][27].

1.2. The Shockley-Queisser limit

In addition to the recombination losses, the conversion efficiency of a solar cell is limited by several factors such as the thermalization losses, the limited lifetime fill factor and the Shockley-Queisser limit [28]. The Shockey-Queisser (SQ) limit (1961) determines which materials are good candidates for designing high efficiency solar cells. Theoretically, a solar cell with the highest power conversion efficiency (PCE) will likewise function as an LED with the highest luminous efficiency. This is because of the complementary action as light emission by radiative recombination is connected to light absorption by the creation of electron-hole pairs via the principle of detailed balance.

The beauty of the Shockley-Queisser SQ approach for the calculation of the limiting efficiency of photovoltaic power conversion is due to the reduction of the solar cell idea to the fundamental physical processes of detailed balance between light absorption and radiative recombination. It takes the black body radiation, the spectrum losses and the recombination

mechanisms into account. It is the cornerstone of the photovoltaic technology and relies on four basic assumptions as described by D. Abou-ras et *al.* [29]: First assumption, for a solar cell under emission of light, the photons with energy greater or equal than the bandgap energy of the material ($E \geq Eg$) could generate a single electron-hole pair after absorption of light while the photons with energy less than the bandgap energy of the device ($E<Eg$) have a zero probability to generate the charge carriers. Secondly, the electron and holes generated after absorption of light by the PV material undergo a thermalization process at the band edges. The third assumption is linked to the generation of charge carriers under illumination of the device at short-circuit conditions. In these conditions, the collection probability is unity. The Shockley-Queisser model involves the principle of detailed balance; therefore, the fourth assumption considers the radiative recombination as main loss mechanism.

By achieving a maximum external luminescence performance, high open-circuit voltages are reached [30]; thus the Shockley-Queisser model enables high solar cell performance for an important luminescent emission of photons and large amount of charge carriers. The detailed balance limit J_{SQ} gives insight on the photocurrent losses and light trapping inside the cell[31][32].

Developing highly efficient, stable and durable solar cells for the photovoltaic market and industry is a key to assess the potential of the technology. For single junction solar cells with a band gap comprises between 0.93 and 1.61 eV, the Fraunhofer Institute for Solar Energy Systems, ISE [33] demonstrated that a PCE of around 30 % is achievable.

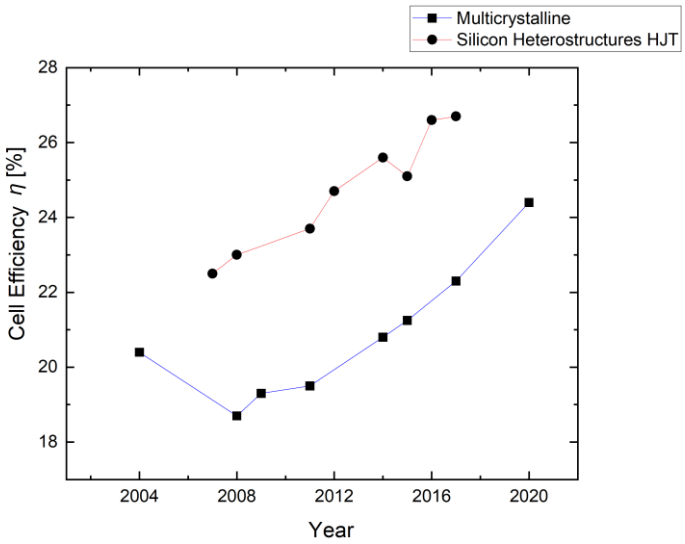

Figure 4: Cell efficiency improvement. Data extracted from[6].

Crystalline silicon heterostructure cells have an updated record efficiency of 26.8 %[6]. A record lab cell efficiency for mono-crystalline and multi-crystalline silicon wafers are respectively 26.7 % and 24.4 % [33]. When comparing the research cell efficiency for multi-crystalline silicon solar cells and silicon heterostructure cells (figure 4), research proves the highest performance for SHT over c-Si and its potential to unlock the PV market.

2. Fundamentals on SHJ and TPC cells

2.1. Silicon Heterojunction solar cell

In the category of crystalline silicon-based solar cells, two main groups of technologies were developed; the homojunction solar cells and the heterojunction solar cells[23]. Practically, SHJ structure uses hydrogenated amorphous silicon combined with crystalline silicon (a-Si:H/c-Si) to reduce the recombination of electron-hole pairs at the interface originated from to the diffused emitter regions, improve the absorption of light by the material and further increase the efficiency of the solar cell device. This combination enables lower temperature processing, lower temperature coefficient and low cost [12]. The a-Si material is well-known for its relatively low-cost but high degree of structural and bonding defects that favors the recombination of holes and electrons and limits the current. In recent years, the conversion efficiency of a-Si based solar cells has remarkably improved [34][35]. Despite the recorded drawback of a-Si and the high degree of defects, some preparation techniques such as PECVD are used to passivate the defects at the interface.

The concept of PN heterojunctions came in response to some previous limitations in the literature like preventing the formation of a Schottky barrier. It results in the combination of diverse materials with different structures, lattice, crystalline/amorphous interfaces. From the texturing and cleaning of the wafer to the deposition of a-Si and Transparent Conductive Oxide (TCO) by PECVD and sputtering respectively and ending by the metallization through screen printing process, the preparation of SHJ cells is flexible. Under illumination, the TCO film layer deposited partially reflects the incident radiation on the cell, the a-Si layer absorbs this incident light and the c-Si wafer absorbs the remaining light for generation of charge carriers and optimized short-circuit current density. Possible candidates of TCO for SHJ front side are ITO, doped ZnO, Ag nanowires, MoO_3/Au/MoO_3 structure, and graphene[36]; however, to guarantee a high transparency, a good conductivity and a low absorption, ITO is commonly

used in SHJ solar cells. It ensures the collection of charge carriers and prevents the diffusion process in the silicon by acting as a diffusion barrier. As an anti-reflection coating layer, ITO film reduces the reflection losses [37]. The rear TCO should meet a high carrier selectivity and low absorption by plasmon.

A representation of the SHJ solar cell used at the study area with the thicknesses of each layer is shown in figure 5. The silver Ag electrodes are used for metal contact.

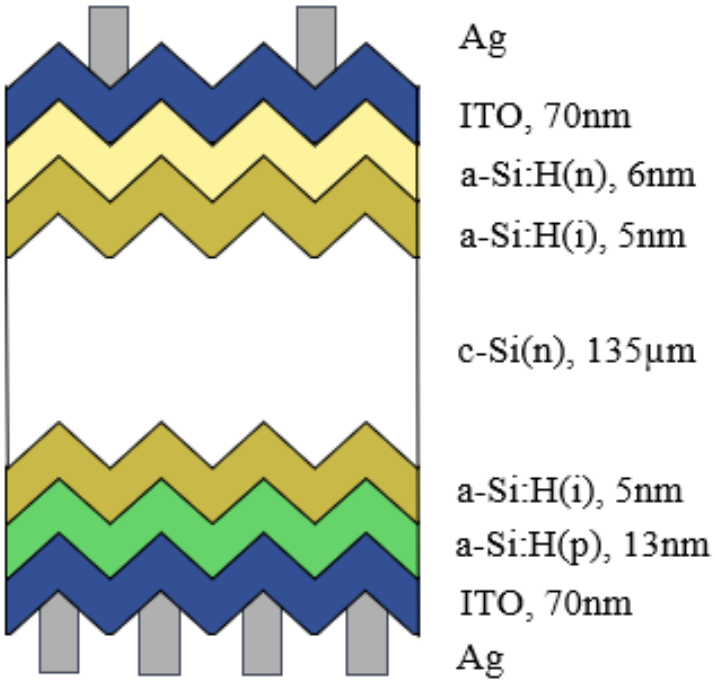

Figure 5: Sketch of the SHJ fabricated at IEK-5

The a-Si:H uses in SHJ can be either n-doped, intrinsic or p-doped. The doping concentrations are 6×10^{21} /cm^3 and 9×10^{19} /cm^3 for a-Si:H (n) and a-Si:H (p), respectively. The epitaxial growth within the cell should be avoided; therefore, the a-Si:H (i) should have a low defect density and surface recombination, and a thermal stability. A key challenge with a-Si:H/c-Si solar cells to achieve lower investment costs is the limitation of the absorption of light due to the thin c-Si wafer used. Furthermore, the reduction of the dangling bond density at the a-Si:H/c-Si interface for high surface passivation was also identified as a challenge[12].

2.2. Transparent Passivating and Conductive Contact solar cells

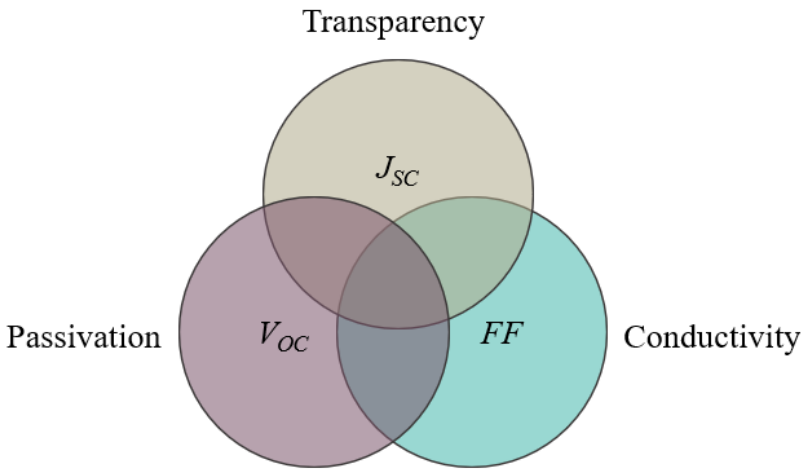

Figure 6: Photovoltaic parameters affecting the performance. Adapted from [38].

As previously mentioned, the TPC approach reduces the recombination losses at the contacts and enhance the performance of the solar cell. The efficiency of the solar cell is determined by the open-circuit voltage V_{OC}, the short-circuit current density J_{SC} and the fill factor *FF*; thus, improving the transparency, conductivity, and passivation of the TPC cell directly contributes to an increase of the efficiency due to the interrelation between them (figure 6).

Passivation can decrease a material's conductivity by preventing charge carriers from reaching the surface or by raising the material's resistance, which is the trade-off between passivation and conductivity. Among the passivating contacts developed early for higher efficiency are the Poly-Si/SiO_x stack solar cells. With this combination identified as TOPCon structure standing for tunnel oxide passivated contacts, recombination losses can be reduced, and the contact quality is improved. Due to the J_{SC} loss in a-Si:H layers, the low bandgaps and absorption coefficients of both poly-Si and a-Si:H, a further development of the passivating contact approach is the TPC concept and the low temperature processes.

By combining microcrystalline silicon carbide µc-SiC:H(n) with a thin layer of silicon tunnel oxide, M. Köhler et *al.* [10] developed a TPC scheme for front side of silicon heterojunction cells without annealing processes and capable of achieving good cell efficiency (figure 7). This c-Si solar cell consisting of TPC as front side and SHJ as rear side is the one considering in this thesis with a particular focus on the TPC surface.

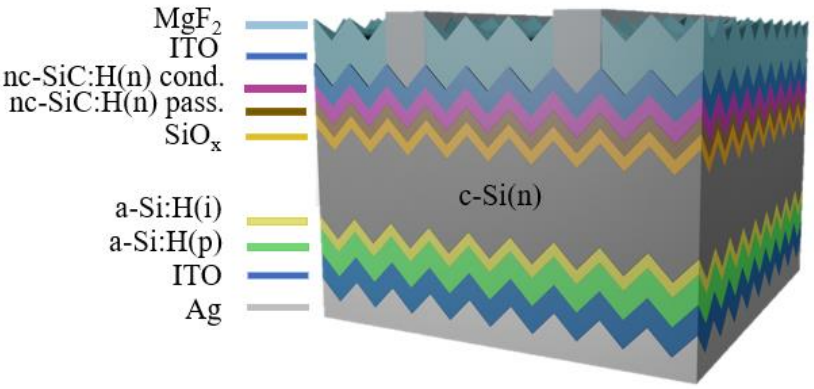

Figure 7: Solar cell investigated with TPC as front side and SHJ as rear side. Adapted from [11].

The TPC structure is fabricated by adding at the top of the n-type doped c-Si(n), a thin layer of silicon oxide SiO_x followed by a double layer of nc-SiC:H(n) deposited by hot-wire chemical vapor deposition (HWCVD). This double layer consists of a passivation layer in contact with the SiO_x layer and a conductive layer at the top of the first one[11]. Further studies done by the authors enable an efficiency of 23.99 % with a J_{SC} of 40.87 mA/cm^{-2} and a fill factor of 80.9%. This TPC concept was optimized in reference [37] and a J_{SC} of 41.21 mA/cm^{-2} was achieved. However, an investigation of the passivation quality after ITO sputtering shows a decrease in the implied open-circuit voltage iV_{OC} in comparison to the final V_{OC} [11]. This has been called "sputter damage" and may arise from the oxygen plasma UV emission or ion bombardment, and may be cured by increasing the ITO deposition pressure [38] or through other curing processes. An assumption from an ongoing investigation is that the sputter damage may originate from the introduction of phonons during the ITO deposition which causes a break in some bonds, leaving more defects.

To improve the three solar cell parameters and thereby the efficiency, the light soaking process was investigated on SHJ solar cells showing an increase of the effective lifetime of the charge carriers due to an improvement of V_{OC} and FF [39]. As the prolonged exposition to light of SHJ used as rear side leads to an increase of the V_{OC}, it may be possible that the light soaking process improves the passivation quality of the investigated TPC structure and cure the sputter damage.

3. Light soaking process

The light soaking effect which means the extended exposure to light, was first experienced in a-Si:H thin films solar cells and called the Steabler-Wronski effect (SWE) [40].

By studying the effect of prolonged exposure to illumination on doped and intrinsic a-Si-H, Steabler and Wronski (1977) observed a reduction of the dark- and photo-conductivity as well as identified some metastable defects in the a-Si:H [41]. It was also demonstrated that the electronic passivation of a-Si:H exhibits an improvement under thermally-assisted light soaking process [42]. Based on the intensity of the illumination, the temperature and the composition of the layers, any solar cell device will show a particular change in the performance and characteristics[43].

The study done by S. Bao *et al.* [42] on the rapidly reversible processes of activation and deactivation in amorphous silicon heterojunction solar cells under extensive light soaking helps to conclude that the extensive light soaking process can further enhance the passivation. Therefore, as the transparent passivating contacts solar cells are strongly affected by the degradation of the passivation quality due to ITO sputtering, it may be advantageous to perform the light soaking on the TPC cells for recovering the passivation quality and thus the improve the performance.

CHAPTER II: MATERIALS AND METHODS

1. Study area

The focus of the present study is on the silicon carbide-based transparent passivating contact double layer surface at the top of the silicon heterojunction solar cell. The mechanism of sputter damage is investigated and the potential of the light soaking process to cure the sputter damage is scrutinized. The study was performed at the Institute for Energy and Climate Research in Photovoltaics (IEK-5 Photovoltaik) of the Forschungszentrum Jülich in Germany.

2. Data collection

In this section, the different tools, materials and experimental methods used for the study are discussed. A description of the methodology steps-by-steps is also provided.

2.1. Materials

For the conduction of the experiments, the materials used are samples and solar cells prepared at the laboratories of the institute IEK-5. Depending on the desired investigation, the materials are: (i) corning EAGLE XG glass with nc-SiC:H, (ii) nc-Si double side polished n-type float zone wafers, (iii) TPC and SHJ symmetric samples, and (iv) TPC and SHJ solar cells. The different materials used are prepared by following some steps and by using some other components as layers such as ITO, a-Si:H and MgF_2.

2.1.1. Fabrication of the solar cells

2.1.1.1. TPC solar cell

The fabrication of TPC solar cell starts by the texturing and cleaning of the Czochralski (CZ) c-Si(n) wafer by Ozone cleaning and a solution of hydrofluoric acid HF is used to remove the content in oxide of the wafer before adding the SiO_x prepared by piranha solution (H_2O_2:H_2SO_4, 60°C). During front side processing, the TPC contact is deposited. Therefore, through hot-wire chemical vapor deposition (HWCVD), the nc-SiC:H(n) double-layer is deposited at the top of the wet-chemically grown SiO_x. The nc-SiC:H(n) layer directly in contact with SiO_x is the passivation layer and the nc-SiC:H(n) layer at the top of the passivation layer is the conductive layer, both prepared at a desired filament temperature T_F measured with a Raytek Marathon pyrometer. The ITO layer is finally prepared by PVD or sputtering. For the

rear side of the TPC solar cell, the SHJ structure is used by depositing intrinsic and p-type a-Si:H (or B-doped) through PECVD. The ITO layer is then sputtered on the a-Si:H(p). For metallization, busbars and fingers fabricated with silver are screen printed on the cell. Some additional layers like MgF_2 can also be deposited by thermal evaporation as a second anti-reflection coating. The composition of the solar cell's layers with different thicknesses is given in Table 1. Through this fabrication processing, the following structure is obtained for the studied cell:

Ag/ITO/ nc-SiC:H(n) cond./ nc-SiC:H(n) pass./SiO_x/c-Si(n)/a-Si:H (i)/a-Si:H(p)/ITO/Ag

Table 1: Composition of the solar cell's layers with corresponding thicknesses[38].

Layers	Thicknesses
MgF_2	125 nm
Front ITO	70nm
nc-SiC:H(n) conductive	30 nm
nc-SiC:H(n) passivating	3 nm
SiO_x	1 nm
c-Si(n)	170 µm
a-Si:H(i)	7 nm
a-Si:H(p)	7.4 nm
Rear ITO	70 nm

The light soaking process can thus be performed on the TPC solar cell to investigate the underlying mechanisms.

2.1.1.2. SHJ reference solar cell

The baseline fabrication of the SHJ solar cell at IEK-5 is similar to the TPC process. At the front side, a stack of a-Si:H (i/n+) is deposited and at the rear side, the a-Si:H (i/p+) stack is deposited both by PECVD technique. The ITO layer is then sputtered on both sides and the silver contacts are screen-printed on the cell. Consequently, the structure of the cell obtained is:

Ag/ITO/ a-Si:H (n)/a-Si:H(i)/c-Si(n)/a-Si:H (i)/a-Si:H(p)/ITO/Ag

For the study, light soaking is also performed on SHJ solar cells after the fabrication process and these SHJ cells are used here for comparison as reference cells since the rear side structure is the same as for TPC solar cells.

2.1.2. Preparation of the symmetric samples

To examine the surface passivation, TPC and SHJ symmetric samples are prepared. For TPC, the structure of the samples is nc-SiC:H(n)/SiO_x/c-Si(n)/SiO_x/nc-SiC:H(n). Equivalently, the SHJ symmetric samples have the following structure: a-Si:H(p)/a-Si:H(i)/c-Si(n)/a-Si:H(i)/a-Si:H(p). The TPC and SHJ symmetric samples are evaluated separately using some characterization methods and represent respectively, the front and rear sides of the finished solar cell.

2.2. Characterization methods

To study the electrical, structural, and optical properties of the TPC solar cells and samples, the following characterization methods are used:

2.2.1. Ellipsometry

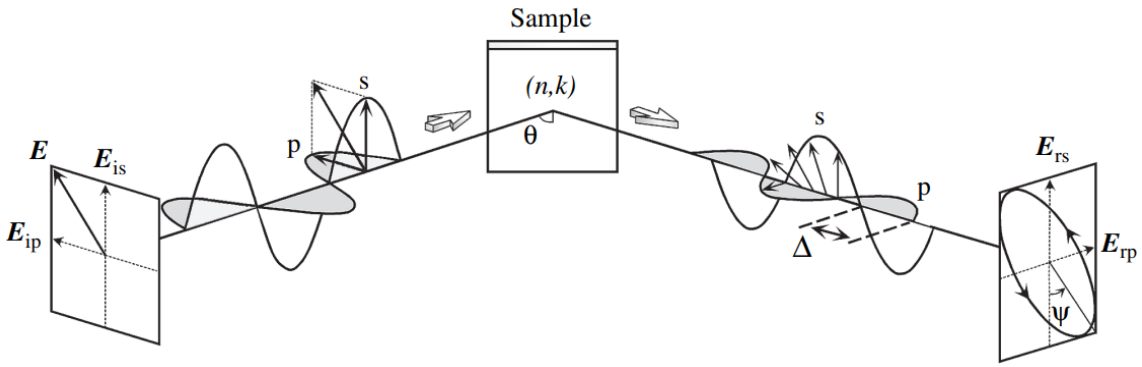

Figure 8: General principle for ellipsometry measurement[44].

Before performing a characterization method on the materials, it is critical to measure the thickness. A general principle of ellipsometry measurement is provided in Figure 8. Since polarized light can be transformed into an ellipse on reflection, the spectroscopic ellipsometry is used, not only to determine the thickness and optical constants but also the doping concentration, the roughness, the crystallinity and visualize the change in polarization ρ of the light represented by an amplitude ratio Ψ and a phase difference Δ. It is also possible to simulate the sample with the modelling option. The mathematical equation describing the ellipsometry parameters is:

$$\rho = \tan(\Psi)\, e^{i\Delta} = \frac{r_p}{r_s} = \left(\frac{E_{rp}}{E_{ip}}\right)/\left(\frac{E_{rs}}{E_{is}}\right) \tag{2.1}$$

$\frac{r_p}{r_s}$ represents the ratio of the amplitude reflection coefficients for p- and s- polarizations, respectively, and $(\frac{E_{rp}}{E_{ip}})/(\frac{E_{rs}}{E_{is}})$ represents the ratio of reflected electric fields to incident electric fields.

The thickness can also be calculated as a function of the deposition rate and times of the layers.

The ellipsometer used at IEK-5 is the J.A. Woollam M-2000 Ellipsometer with automated angle, high accuracy and precision. It allows the measurement of spectra from ultraviolet to near infrared. To start, the power source is turned on and the lamps are ignited. Then, the samples are placed on the sample stage with the vacuum turns on to hold the sample in place, and the light beam are adjusted with the center of the sample. The next step is the measurement with the software CompleteEASE after defining the recipe, the data acquisition parameters and the high accuracy mode. With the value of the thickness, more accurate characterization techniques can be performed such as conductivity measurement.

2.2.2. LOANA Solar cell analysis system

The LOANA solar cell analysis system is a device analysis system which provide various information about the solar cell measured from the *J-V* characteristics to the external quantum efficiency EQE, the reflectance R, and the defects in the cell through electroluminescence EL measurement. It is also possible to localize the shunts, investigate the recombination losses through lock-in thermography, the doping concentration with capacitance-voltage measurement and the busbar-to-busbar resistance. The system is made up of a supply unit, a sample compartment and a control rack unit. The supply unit consists of a monochromatic light source (a 250 W Tungsten halogen lamp, a 300 W Xenon arc lamp and a fully automated grating monochromator), a bias light source, a vacuum pump, a thermostat and some power supplies. In the sample compartment, an xyz measurement table with cameras (EL, IR and microscope), optics and motor ensure the possible measurement of the device parameters. The control rack consists of a PC with console to visualize the different measurements, an emergency stop button, some control electronics to monitor the system.

To simulate the TPC solar cell device with the LOANA system, several methods are used. However, only the different methods performed during the study are presented here.

2.2.2.1. *J-V* measurement

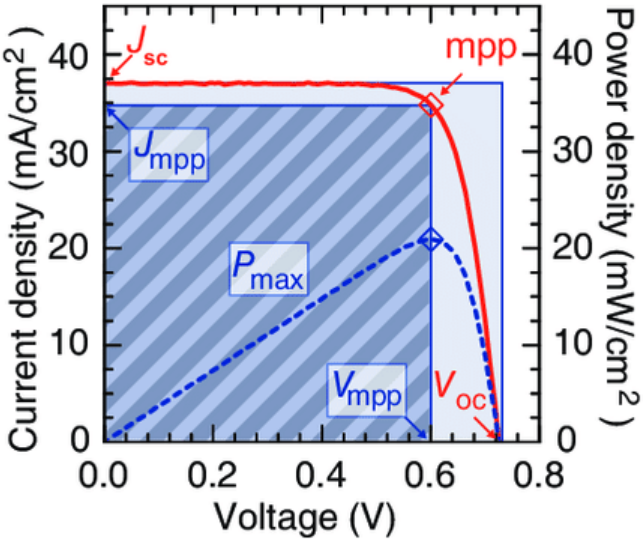

Figure 9: Example of *J-V* and *P-V* curves for a solar cell. Adapted from [45].

In characterizing the TPC solar cell, the *J-V* measurement refers to an efficiency measurement of the cell such as the efficiency η (%), the short-circuit current density J_{SC} (mA/cm^2), the open-circuit voltage V_{OC} (mV), the fill factor *FF* (%) and the series resistance R_S (Ω cm^2).

To start the measurement of the TPC cells (area A = 4 cm^2) with LOANA, the required components for small cells like the lamp mask, the chuck and the contact frame are connected, and the sample is placed on the chuck. Then, the operator can fill out the information on the measurement (recipe, structure of the sample, type of chuck, sample name, lot, etc.) in the PC connected to the control rack unit of the system. Before each measurement, it is required to do the pin check to ensure a good contact at the back side. With this system, it is possible to perform dark- and illuminated- measurements. Therefore, one can measure the *J-V* dark, J_{SC}-V_{OC} and *J-V* light. The results are collected and analyzed using the PV tools CELLIE, PIXIE, and TRACIE.

The parameters measured shown in figure 9 are obtained through mathematical calculations. The efficiency η is the ratio of the electrical areal cell power at maximum power point (MPP) divided by the optical areal input power of AM1.5 spectrum:

$$\eta_{cell} = \frac{P_{MPP}}{P_{in}} = \frac{J_{MPP} V_{MPP}}{P_{in}} \quad (2.2)$$

The maximum output power P_{MPP} is equal to the current density times the voltage both at maximum power point. The cells are measured under standard testing conditions (STC) which correspond to an irradiance of 1000 W/m^2, a temperature artificially maintained at 25 ℃ and an artificial AM1.5G spectrum. Therefore, the input power P_{in} is equal to 1000 W/m^2.

The short-circuit current density J_{SC} of the cell is the current I_{SC} per unit of area A measured when the voltage is at zero:

$$J_{SC} = \frac{I_{SC}}{A} \tag{2.3}$$

The *J-V* curve is described by the following solar cell equation:

$$J = J_0 \left[\exp\left(\frac{qV}{n_{\mathrm{id}}kT}\right) - 1\right] - J_L \tag{2.4}$$

Where J_0 is the dark saturation current density which represents the recombination current in the solar cell, J_{L} the light generated current density, q the charge carrier, V the Voltage, n_{id} the ideality factor, k the Boltzmann constant and T the Temperature of the cell.

During J_{SC}-V_{OC} measurement, the *J-V* characteristics are measured in the absence of series resistance and the J_{SC}-V_{OC} curve is obtained for different light intensities. At short-circuit conditions, the solar cell equation becomes:

$$J = J_0 \left[\exp\left(\frac{qV}{n_{\mathrm{id}}kT}\right) - 1\right] - J_{\mathrm{SC}} \tag{2.5}$$

The open-circuit voltage V_{OC} or maximum possible voltage produced by the cell is obtained through the equation:

$$V_{\mathrm{OC}} = \frac{n_{\mathrm{id}}kT}{q} \ln\left(\frac{J_{\mathrm{SC}}}{J_0} + 1\right) \tag{2.6}$$

This expression of V_{OC} is derived from the Shockley diode equation. During the efficiency measurement, one can also measure the fill factor *FF* which is defined as the ratio of the maximum power of the cell to the product of J_{SC} and V_{OC}. It is graphically a measure of the squareness of the solar cell.

$$FF = \frac{J_{\mathrm{MPP}}V_{\mathrm{MPP}}}{J_{\mathrm{SC}}V_{\mathrm{OC}}} \tag{2.7}$$

One last important parameter obtained by *J-V* measurement is the series resistance. As described in the previous chapter, the series resistance can be evaluated at maximum power point from the pseudo-fill factor *pFF*:

$$R_S = pFF - FF \tag{2.8}$$

The pseudo-fill factor is determined from the Suns-V_{OC} curve which is beneficial since the Suns-V_{OC} relies on a cell's voltage to be measured. Consequently, it may be carried out directly on the ITO without the use of metal connections.

2.2.2.2. Electroluminescence imaging

The electroluminescence imaging setup integrated in the LOANA system is used to inspect the optical properties of the solar cell but also the recombination of charge carriers, the local series resistance, and other defects (broken fingers, contact issues, etc.) in the bulk of the solar cell using a light emitted signal and a CCD (Charge Coupled Device) camera. The characterization of TPC cells by EL is performed through consecutive calibration images of each of the four solar cells fabricated on the 7.8 x 7.8 cm^2 c-Si wafer. A schematic representation of the setup is presented on figure 10 (right). The finished TPC solar cell device fabricated at the study area is shown in figure 10 (left).

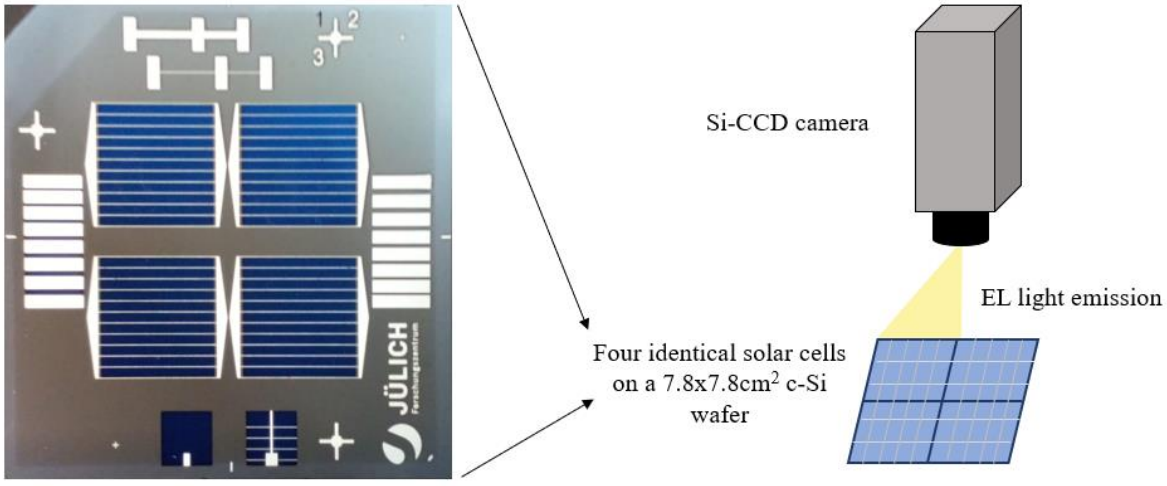

Figure 10: EL imaging setup for characterizing the finished TPC solar cell

The EL response depends on the quantum efficiency close to the band gap [46] as described by the reciprocity theorem :

$$\phi(E) = EQE(E)\phi_{bb}(E)\left[e^{\frac{qV}{kT}} - 1\right] \tag{2.9}$$

Where ϕ(E) represents the EL intensity and depends on the external quantum efficiency EQE(E), qV the split of the quasi-Fermi levels, $\phi_{bb}(E)$ the black body radiation and kT the thermal energy.

EL was performed together with *J-V* measurement to better visualize the possible changes inside the cells after light soaking and the images are presented in Appendix B.2.

2.2.3. Quasi-Steady state photoconductance

The passivation quality of TPC solar cells is studied via quasi-steady state photoconductance (QSSPC) lifetime measurement. For this, the implied open circuit voltage is measured at 1-Sun. Its foundation is the inductive coupling of a semiconductor sample to an RF bridge circuit through a coil, the output voltage of which is linearly related to the measured sample's photoconductance. This technique uses a high-intensity flash to generate an electron-hole pair within the material to allow the determination of the effective carrier lifetime corresponding to the time needed for the charge carriers to undergo a recombination process or other optical losses.

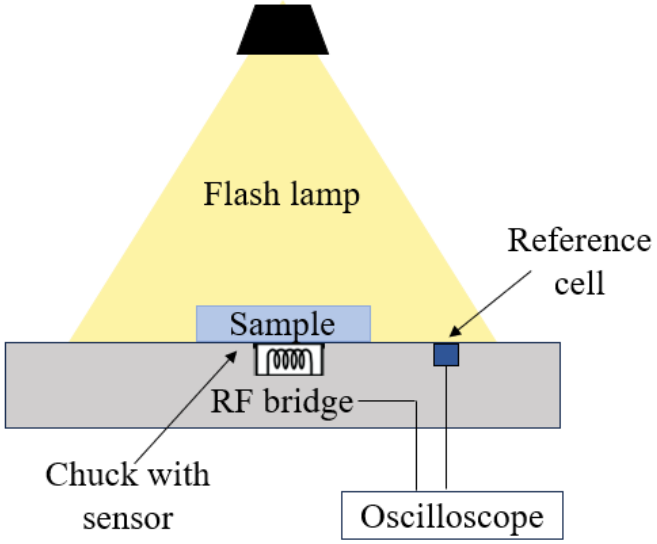

Figure 11: QSSPC setup

In this thesis, the QSSPC setup (figure 11) was mainly used for iV_{OC} measurement and injection-dependent carriers lifetime change of different samples. The sample is placed on the sensor and the passivation quality as well as the effective carrier lifetime is investigated under flashlight decays during a few seconds. As found in the literature, the implied V_{OC} is calculated

as a function of the generated excess charge carriers Δn and the intrinsic carrier densities n_i and N_A:

$$iV_{OC} = \frac{k_B T}{q} \ln\left(\frac{\Delta n(n+N_A)}{n_i^2}\right) \quad (2.12)$$

2.2.4. Electrical characterization

To scrutinize the electrical resistance of the nc-SiC:H(n) material, two main electrical characterization methods were used and are presented in this part; the conductivity measurement with evaporation of silver as contacts and the transmission line method (TLM) also called transfer length method. The electrical characterization is performed to better analyze the fill factor and the series resistance of the TPC solar cell.

2.2.4.1. Conductivity

The electrical resistance between two silver contact points deposited on the nc-SiC:H (n) layer is performed via a two-point measurement setup (Figure 12). For this, the SiC samples prepared on corning glass (CG) are cut with a glass cutter system to meet a requirement of 10 x15 mm^2 area for the two-point conductivity measurement. After cutting the samples, the next step is to deposit two silvers contact pads at the front side of nc-SiC:H(n) by evaporation to create a conductive ohmic contact. The silver contact pads deposited on the samples have a length of 5 mm and the distance between two contacts is 0.3 mm.

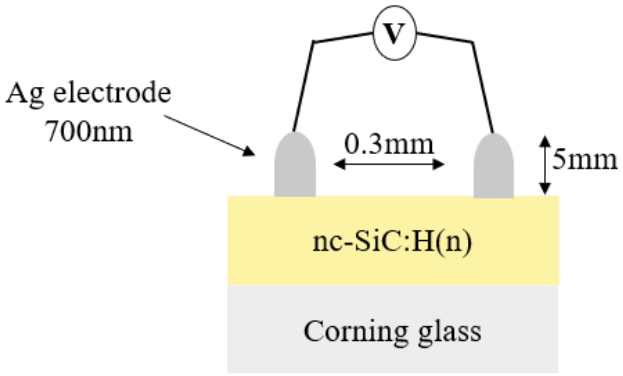

Figure 12: Setup for a two-point conductivity measurement

After evaporating the silver contact onto the nc-SiC:H(n) layer, the measurement is performed under three conditions: (i) dark conditions (ii) under a fixed temperature of 293 K and (iii) in vacuum to minimize the contributions of any external gases or contaminants. The conductivity is thus measured by connecting the two contact pads to the measurement setup and

by applying a voltage V. The current J that passes through the sample is measured. Since the contact between the silver electrodes is ohmic, the value of conductivity ($\sigma = \frac{1}{R}$) is obtained using the Ohm's law ($R=V\times I$) and can be expressed as [47] :

$$\sigma = \frac{J}{V}\frac{L}{Wd} \tag{2.13}$$

With: J the lateral current, V the voltage applied, L the length of the contact pads (5mm), W the width and d the thickness of the nc-SiC:H (n) layer measured by ellipsometry.

2.2.4.2. Transmission Line Method

Another electrical characterization method is the transmission line method which is used to investigate the contact resistivity between Ag and the TPC n-type stack $\rho_{C\ Ag/TPC}$ (Figure 13, left) as well as the contact resistivity between ITO and the Ag metallization $\rho_{C\ Ag/ITO}$ (Figure 13, right). Here, the resistivity of only Ag/ITO contact is studied. To obtain the desired values, a voltage is applied between the two silver contact pads and the corresponding JV curve is measured for each distance between the contacts.

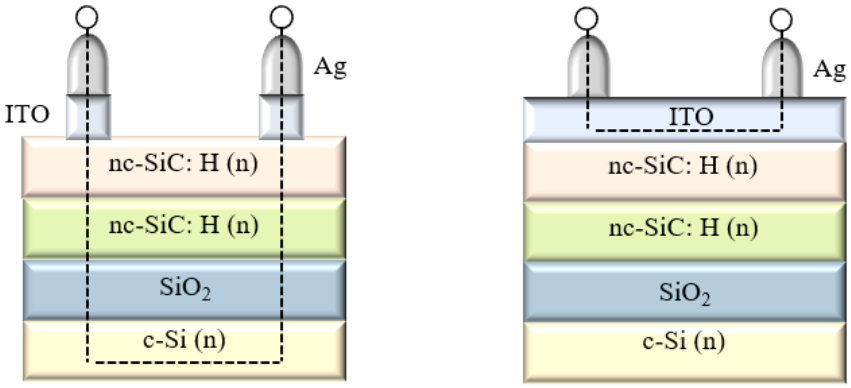

Figure 13: TLM measurement for Ag/TPC n-stack (left) and Ag/ITO interface (right)

With a linear fit of the Resistance-Distance R(d) curve, the contact resistance R_c (x=0; y=$2R_c$) and the transfer length L_T (x=$-2L_T$; y=0) are obtained. The slope of this curve gives insights on the sheet resistance R_{sh} which is also linked to the transfer length:

$$L_T = \sqrt{\frac{\rho_c}{R_{sh}}} \tag{2.14}$$

The contact resistivity is calculated using the relation:

$$\rho_c = R_c L_T W \tag{2.15}$$

2.2.5. FTIR spectroscopy

The nanostructure of silicon carbide is characterized by Fourier Transform Infrared (FTIR) spectroscopy. It uses a Fourier transform algorithm to deliver the spectra of the material. As the nc-SiC:H(n) was deposited by HWCVD on the silicon wafer, the composition of the sample is studied through IR light emission. The spectrometer used is the Nicolet 5700 spectrometer by Thermo Electron Corporation. It consists of three compartments (detector compartment, cell compartment, beam splitter and desiccant compartment) connected to other external components such as the external source emission port, the external beam hole, and holes for filling detector. At the upper level of the spectrometer, the status indicators and data collection buttons are used to monitor the system manually and the sample is inserted via a movable door. The principle of the measurement is presented in figure 14. The FTIR spectrometer used during this study is connected to a computer system for an automatic collection of data and monitoring of the system. In addition to chemical composition analysis, the FTIR spectroscopy was used to analyze the effect of light soaking on the absorbance of the material under IR radiation.

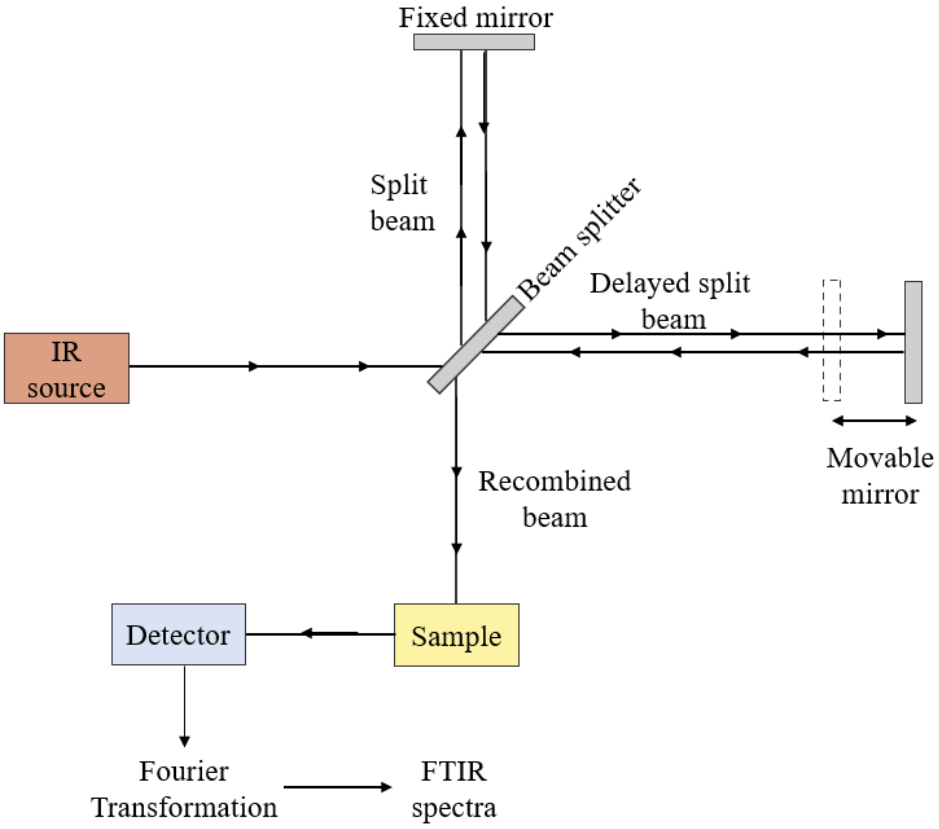

Figure 14: FTIR principle of measurement

2.2.6. Light soaking system

The light soaking system (LiSo) used for this study is produced by Gsolar and is sketched in figure 15. It consists of three compartments (sample or pre-treatment compartment, heating chamber, and post-treatment compartment) and functions with automatic robots. The cells are inserted in the pre-treatment compartment on a rail system which brings the cells, four by four, in the light source compartment. The power of the LED panel light is 55 kW/m^2.

To cool down the system due to the very high intensity of light and heat, a water-cooling system is connected to the oven. The duration of the light exposure can be manually set and to keep a desired temperature inside the system, it is possible to define the temperature of the heating table and the process temperature. A pyrometer and a PT100 are therefore used for the temperature control. The different chambers are made of glasses and mirrors for preventing overheating and optical losses respectively.

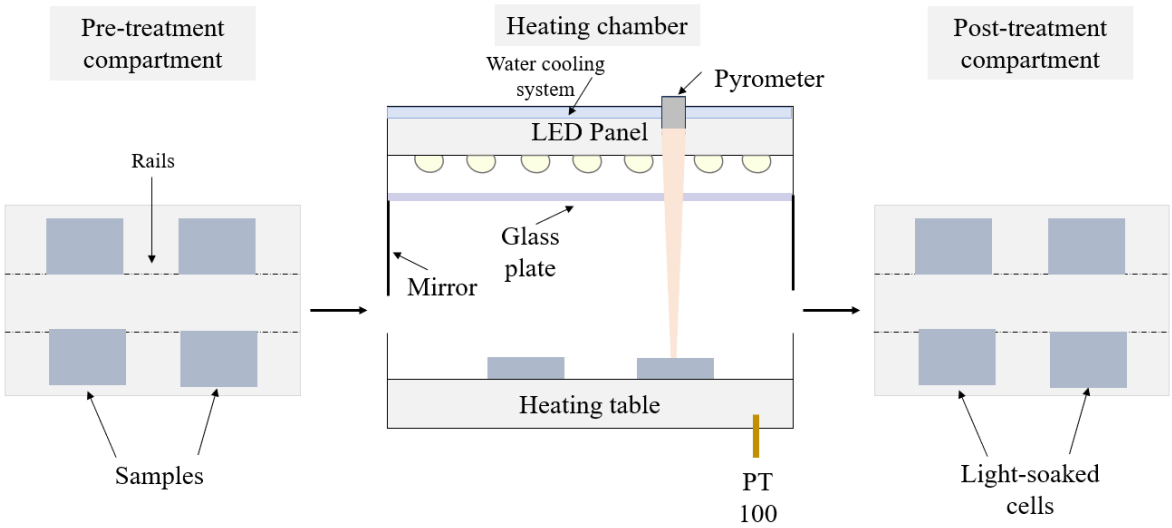

Figure 15: Light soaking system at the study area

After the treatment time, the cells are transferred to the last compartment and removed from the rail system by the robots. This setup used at IEK-5 was firstly studied by T. Rudolph [47] and a detailed presentation of the system as well as the spectrum characterization is provided. Various characterization techniques can be performed on the light-soaked cells to analyze the effect of extended exposure to illumination on the photovoltaic parameters and more specifically on the passivation quality for TPC cells.

3. Data analysis

The data processing and analysis during the study were possible using some software connected to or independent of the systems and equipment used for the measurements. The results were analyzed as numerical values, curves, graphs, or images.

3.1. PV tools: CELLIE, PIXIE, AND TRACIE

The collection and analysis of the data obtained with the LOANA system are done with the three PV-tools software CELLIE, PIXIE and TRACIE. The software TRACIE helps to visualize in 2-D the curves and graphs plotted by the system during the measurements (*J-V* dark, *J-V* light, EQE, etc.) to compare and evaluate them. In defects investigations, PIXIE particularly ensures an evaluation of the sample images provided by the cameras. With the software CELLIE also called the LOANA database, it is possible to visualize and collect the data measured numerically by the system in columns that can be used in other software to plot the graphs or create reports.

3.2. CompleteEASE software

For the ellipsometry measurements of transparent films, the data analysis is facilitated with the software CompleteEASE of J.A Woollam. The software is used for measurement, in-situ monitoring and process control, data analysis and modelling. Visualizing the data (thickness and roughness) as a map with scale and error bars is also possible. In the case of thickness measurement, it is necessary to adjust the roughness to obtain a more accurate value for the sample.

3.3. OriginLab

All the graphs and curves of the present study were plotted using the software OriginLab which is a professional and easy tool to transform numerical data into graphics.

4. Methodology

The experimental study started by an investigation of the sputter damage causing the degradation of the passivation. Then, the light soaking treatment were performed under different conditions including the exposure duration, the low or high process temperature and the synergistic or independent contributions of heat and light. The effect of light soaking on the

TPC solar cells and symmetric samples was examined through the characterization methods. Furthermore, the results obtained were compared with the baseline works and other studies. Lastly, the structural and electrical properties of nc-SiC:H(n) was studied with a particular interest of the change after ITO sputtering. Based on these investigations, conclusions are drawn on the influence of light soaking treatment on TPC solar cells and a better understanding of the underlying mechanisms is provided.

CHAPTER III: RESULTS AND DISCUSSIONS

In this chapter, a presentation of the results obtained during the experimental methods and data collection is given. Discussions and analysis of the results are provided in light to the research problem.

1. Sputter damage on TPC solar cells

The degradation of the passivation quality during the TPC solar cell fabrication process is mainly due to the sputter damage during ITO deposition before metallization. To better understand the sputter damage, the change of the passivation, from the cell precursor to the TPC solar cell, was investigated. Before ITO sputtering and any metallization contact formation by screen-printing, the initial implied open-circuit voltage (iV_{OC}) of the precursor measured by quasi-steady state photoconductance is around 742 mV. After ITO sputtering on both sides, the QSSPC measurement reveals a drop of the iV_{OC} from the initial value of around 742 mV to 714 mV (Figure 16). This result highlights a degradation of the passivation quality due to the sputter damage. Here, the difference between the initial implied iV_{OC} and the final V_{OC} is 28 mV.

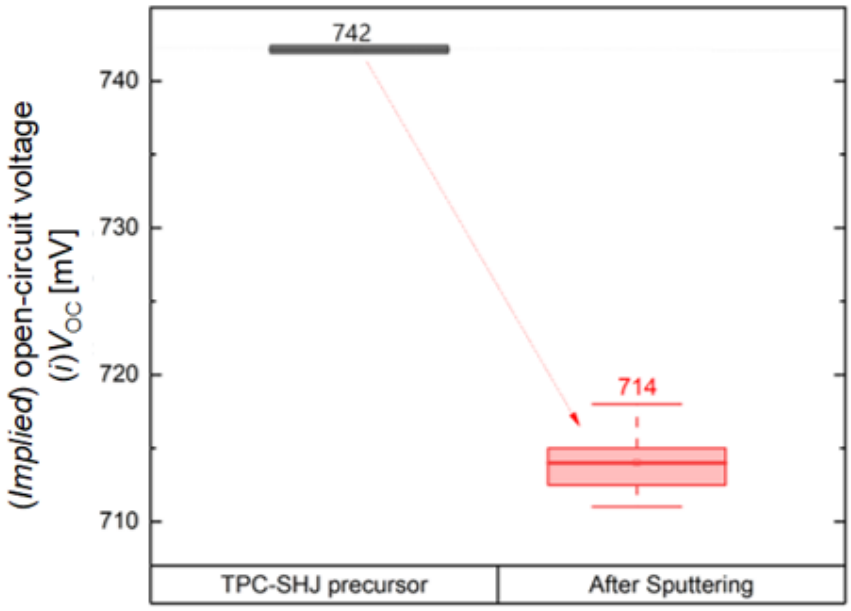

Figure 16: Sputter damage identification on TPC-SHJ solar cell

A first identification of the mechanism of sputter damage was done by M. Köhler et al. [11] and the results align with the ones obtained here. In this study, a difference of 32 mV between the initial iV_{OC} and the final V_{OC} after ITO sputtering was recorded, and the sputter

damage was investigated through effective minority carrier lifetime of two TPC symmetric samples exposed to a 1.5 – 5 % oxygen plasma. The characterization method used was the photoluminescence imaging before and after exposure to the plasma and ITO sputtering. From this experiment, it was concluded that the exposure to 15 min plasma and the deposition of ITO on the TPC symmetric samples deteriorates the passivation quality. A. H. T. Le *et al.* [48] mentioned that the change in effective lifetime of charge carriers after ITO deposition is mainly affected by ion bombardment, the luminescence of the sputtering plasma and the process temperature in or after ITO sputtering. Many studies focused on the deposition rate and parameters for ITO sputtering to reduce the V_{OC} loss. In SHJ cells, higher deposition temperatures of ITO were found to increase the open-circuit voltage V_{OC}, the fill factor *FF* and the short-circuit current density J_{SC} resulting from an improvement of the passivation quality, the conductivity and the transparency of the ITO layer [49]. Therefore, alternatives such as the annealing process at high temperature to cure the sputter damage and charge carrier lifetime degradation were tested in the investigated TPC solar cell.

Here, the sputter damage is thus cured on a hot plate for pure thermal annealing treatment during 20 min at 230 °C. An improvement of the *V*oc to around 718 mV is observed, which is still lower than the initial iV_{OC} for the TPC-SHJ precursor studied. The difference is recorded to be 24 mV.

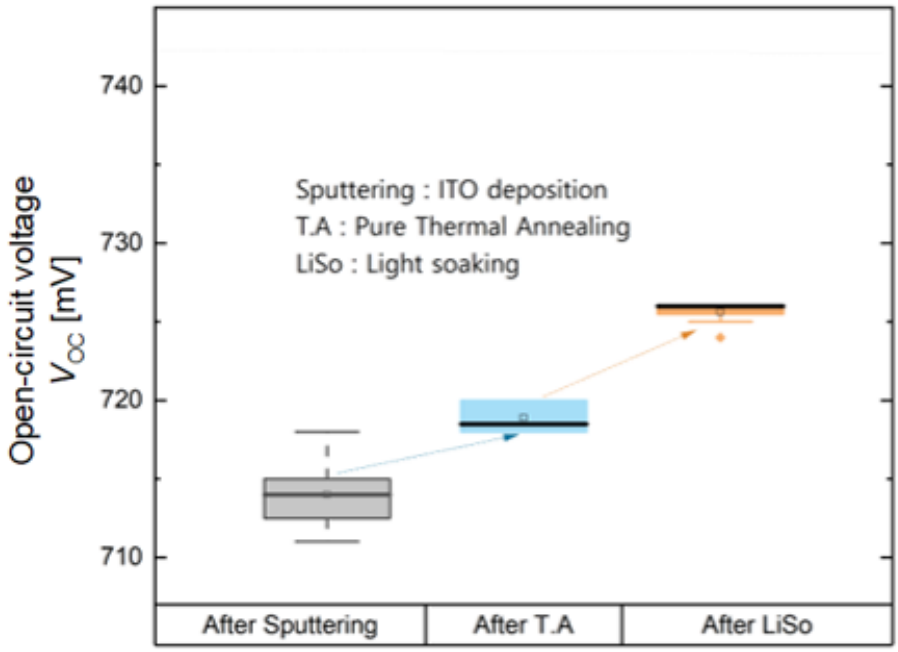

Figure 17: Post-curing treatments of sputter damage on TPC solar cell

By combining the thermal and illumination effects for the improvement of the power conversion efficiency in SHJ solar cells, T. Rudolph [47] investigated a thermally-assisted light soaking treatment on SHJ solar cells which further increased the V_{OC} thus the passivation quality. As the prolonged exposition to light of SHJ-SHJ cells leads to an increase of the effective lifetime of the charge carriers due to an improvement of V_{OC} and FF, it could be possible that the light soaking improves the passivation quality of the investigated TPC-SHJ structure and cure the sputter damage. So, a second possible curing option for TPC cells is the light soaking process.

After the previous thermal annealing, the samples are then cured through a heat-assisted light soaking during 90 s using the recipe of SHJ. Results showed an increase of the V_{OC} to around 725 mV which further improves the passivation quality than the thermal curing. Figure 17 presents the results explained for pure thermal annealing and then further for light soaking curing of the sputter damage. As thermally assisted light soaking involves different parameters and conditions of use, the light soaking treatment without pre-annealing process and its potential to cure the sputter damage on TPC solar cells needs therefore to be better investigated.
In the following sections, the different investigations and results for the curing of TPC symmetric samples and TPC solar cells with direct light soaking are discussed.

2. Direct light soaking treatment of TPC symmetric samples

The TPC symmetric samples are prepared to simulate the front side of the solar cell and monitor the change in iVoc. Two parameters influence the light curing process: the duration of light exposure and the temperature of the heating process. To define the appropriate conditions (duration and temperature) for direct light soaking on TPC solar cell, some experiments were conducted on the symmetric samples for surface passivation evaluation. First, the suitable duration was investigated; therefore, the effect of fast to long exposure to illumination on the passivation quality at a fixed temperature of 175 °C is analyzed. For each treatment steps, the implied open-circuit voltage measured by QSSPC is recorded (Figure 18).

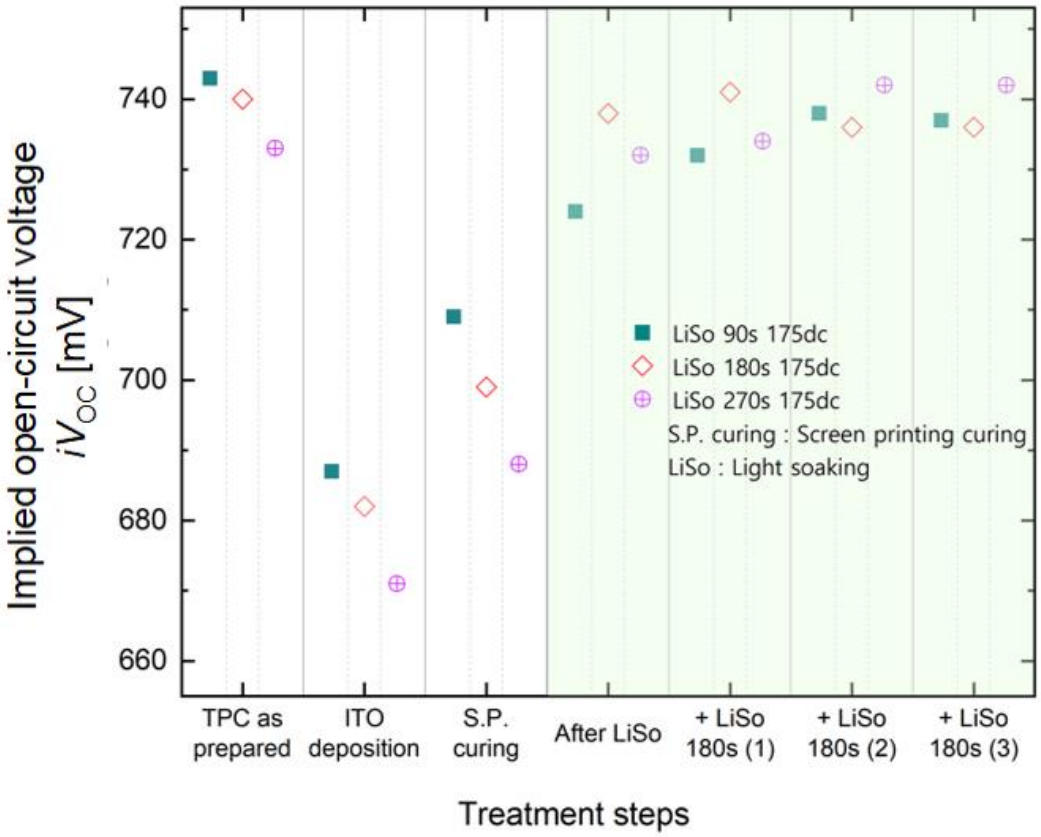

Figure 18: Passivation quality evaluation for TPC symmetric samples under fixed process temperature

Three durations are set: (i) fast light soaking 90 s (ii) light soaking at 180 s (iii) light soaking at 270 s. After a first light curing on the three different samples, three consecutive treatments of 180 s each are performed to see whether the extended exposure to heat-assisted light soaking can fully recover the passivation quality. Results show that after only 180 s+180 s (360 s), the passivation quality is fully recovered but for a prolonged exposure above 360 s, there is a loss of the iV_{OC} indicating a re-deterioration of the passivation quality. In another hand, a remarkable increase of the iV_{OC} was also obtained after 270 s + 2-times 180 s LiSo; however, since the accumulation of heat weakens the samples, it is concluded that the exposure duration of 360 s is suitable for improving the passivation quality of TPC symmetric samples and thereby, of TPC solar cells.

The suitable process temperature is also evaluated in a similar way. During the heat-assisted light curing, the final process temperature depends on the heat coming from the light source and the heating table. By separating the contribution of heat and light during the experiment, it is possible to conclude on the possible necessity to operate with or without light,

at low or high temperature. For this purpose, at a fixed pre-defined process duration of 360 s, three sputter damaged symmetric samples were each cured at respectively (i) 30 ℃ for low temperature curing (ii) 175 ℃ for heat-assisted light curing and (iii) 175 ℃ without light for heat-assisted dark curing equivalent to the annealing process. Figure 19 shows the results of the experiments.

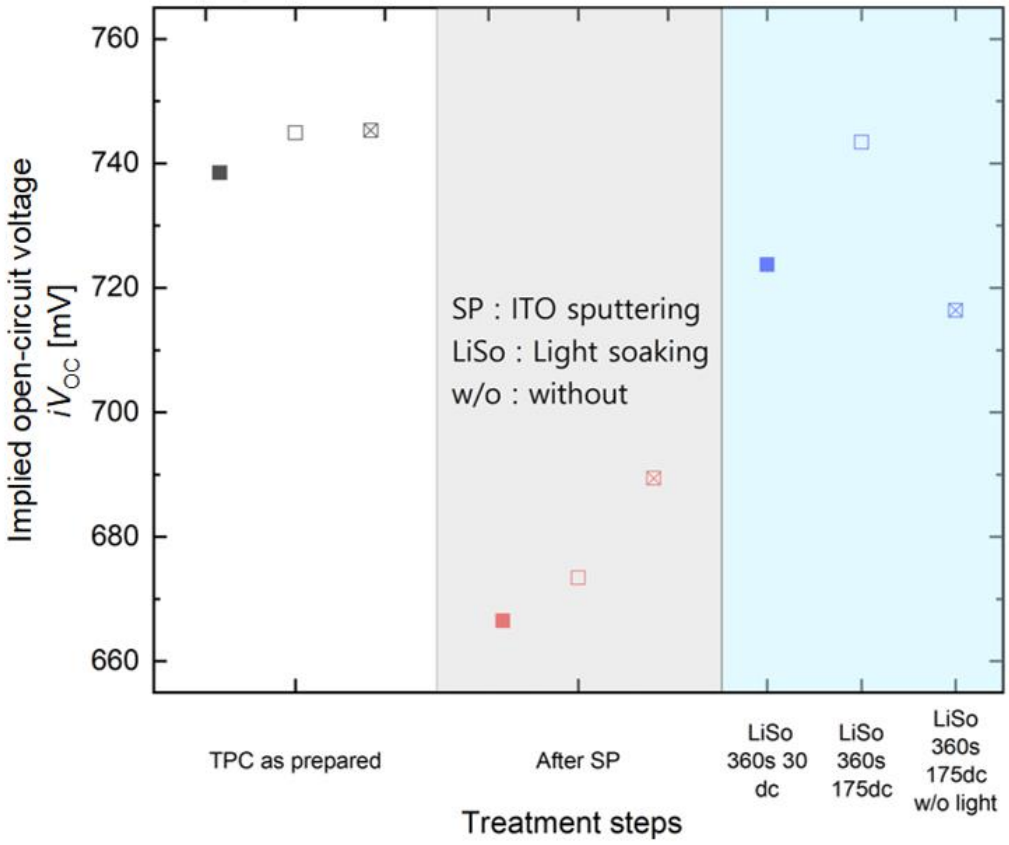

Figure 19: Passivation quality evaluation for TPC symmetric samples under fixed process duration

The combination of heat from the heating table and the light source is found to be an important condition to fully recover the passivation quality. At low temperature, the V_{OC} loss after ITO sputtering is reduced but is not sufficient to fully recover the initial value although the results obtained are better compared to the treatment without light. When the light source is turned off (heat-assisted dark curing), only 27 mV is recovered against 70 mV for the heat-assisted light curing and 57 mV for low-temperature light curing. Therefore, it can be stated from the two previous results that the suitable parameters to characterize the direct light soaking

on TPC solar cells are: (a) an exposure time of 360s and (b) a heat-assisted light curing process for a temperature of 175 ℃.

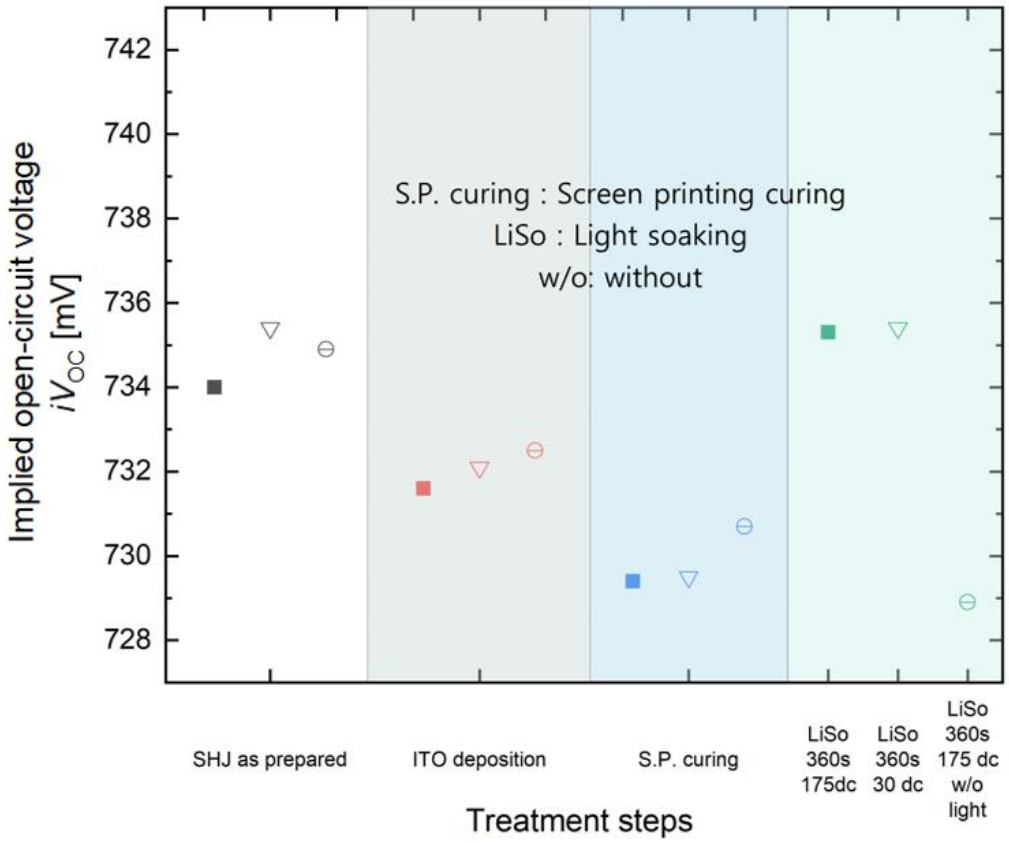

Figure 20: Passivation quality evaluation for SHJ symmetric samples

The rear side structure of the TPC solar was also investigated by preparing SHJ symmetric samples and recording the change in iV_{OC} after each treatment steps (Figure 20). It is concluded here that the direct heat-assisted light soaking curing fully recover the passivation quality and the low temperature light soaking has the potential to cure the sputter damage.

The recipe for direct light soaking curing for TPC and SHJ solar cells are presented in Table 2 and will be taking into account in the next investigations.

Table 2: Direct light soaking recipe for SHJ and TPC solar cells.

Cells	Duration	Temperature	Dark/light
TPC	360 s	175 ℃	Light
SHJ	90 s	175 ℃	Light

3. Direct light soaking treatment of TPC solar cells

In this section, the effect of direct light soaking process on the TPC solar cells parameters is studied. The results are obtained through *J-V* measurement with the LOANA solar cell system analysis. During the experiments, both QSSPC and *J-V* measurements of the TPC symmetric samples and the TPC solar cells are done, respectively, in order to simultaneously compare the change in open-circuit voltage V_{OC} with measured implied open-circuit voltage iV_{OC} and to investigate the behavior of the three other photovoltaic parameters affecting the efficiency of the solar cell which are the fill factor, the series resistance and the short-circuit current density.

3.1. Analysis of different light soaking curing on TPC solar cells

In characterizing the direct heat-assisted light soaking on TPC solar cells and confirm whether this mechanism is a promising way to develop high efficiency TPC solar cells by curing the passivation loss due to ITO deposition, different experiments were conducted as similar as previously. First, the change in η, V_{OC}, FF, J_{SC} and R_S of the TPC solar cells are examined under the three direct light soaking conditions pre-defined to separate the contributions of heat and light during the curing process. The results are presented and discussed individually.

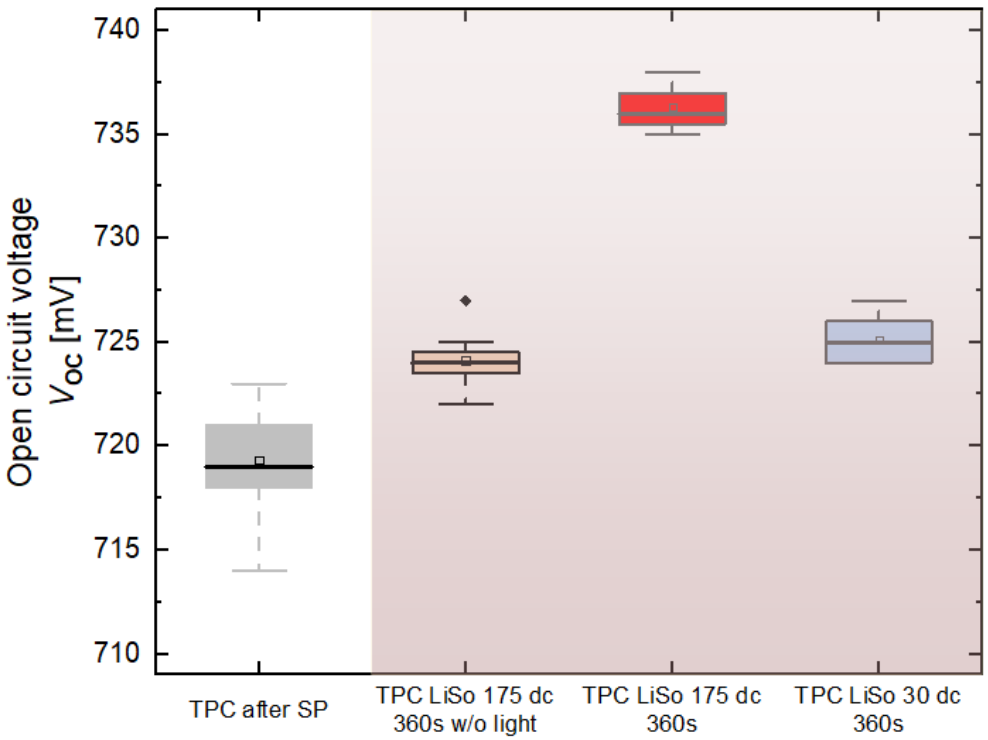

Figure 21: V_{OC} variation for TPC solar cells under different LiSo conditions

The evolution of the V_{OC} after direct light soaking is shown in figure 21. The passivation quality is strongly improved with normal light soaking on TPC solar cells, although not completely recovered as observed with the TPC symmetric samples in the same conditions. The result confirms that the synergistic effect of heat from the heating table and the light source contributes to the achievement of a better V_{OC} and good surface passivation.

The final open-circuit voltage of the TPC solar cell after light soaking is around 736mV which is quite close to the initial iV_{OC} value of 740mV. The low V_{OC} recovering results obtained at both low temperature light soaking and heat-assisted dark light soaking are analogous to the results obtained with the tested symmetric samples and justified the need to operate light soaking at the standard conditions highlighted.

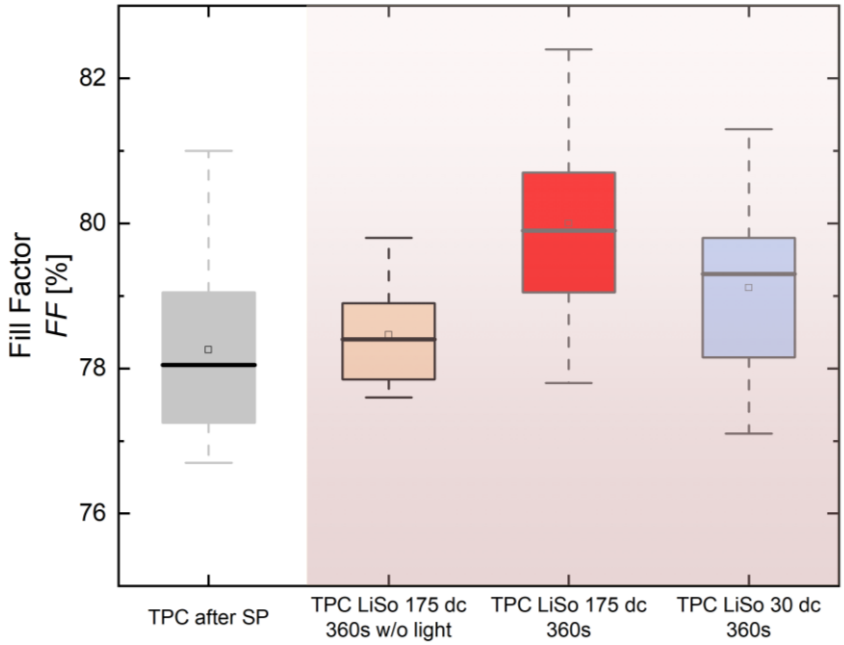

Figure 22: *FF* variation for TPC solar cell under different LiSo conditions

The fill factor of the TPC solar cell measured after SP (as prepared, after ITO sputtering and screen printing) is 78.25%. After direct light soaking applied on the cell (figure 22), the fill factor is 78.46% with heat-assisted dark curing, 80% for normal or heat-assisted light soaking and 79.11% for low-temperature light soaking, respectively, which endow an achievement of high conductivity with standard light curing conditions.

Another parameter affecting the conductivity of the cell is the series resistance. The lower the series resistance, the higher the fill factor and thus the good possible conductivity. As

presented in figure 23 below, the lowest series resistance (R_S = 1.146 Ω cm^2) is also achieved at normal heat-assisted light soaking. After ITO sputtering, the initial series resistance was R_S = 1.245 Ω cm^2. In order to better investigate the effect of direct light soaking on the electrical properties of TPC solar cell, further experiments on conductivity and contact resistivity were performed and are discussed in the next sections.

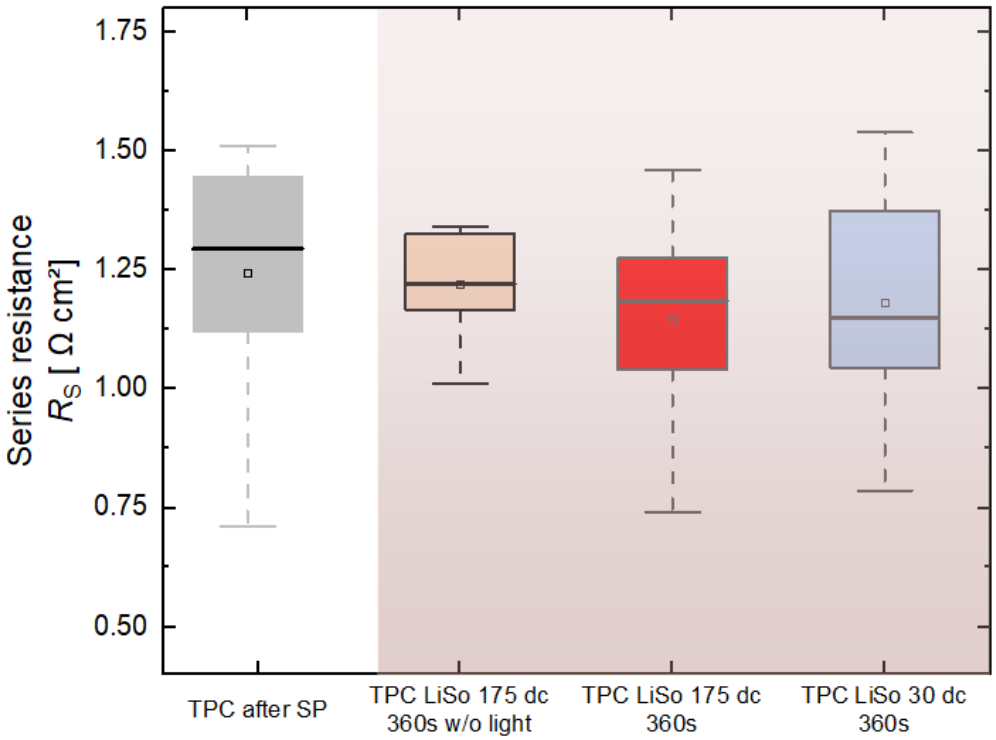

Figure 23: R_S variation for TPC solar cell under different LiSo conditions

An important performance parameter when it comes to the generation of electric current by the TPC solar cell is the short-circuit current density J_{SC}. Previous studies done on TPC enable an achievement of J_{SC} around 41 mA/cm^2. In the development of a TPC concept for the front side of SHJ solar cell done in [11], a J_{SC} value of 40.87 mA/cm^2 was obtained for the finished solar cell. An optimization of the same TPC cell with an additional anti-reflection coating made of ITO, Si_3N_4 and MgF_2 gave a short-circuit current density of 41.21 mA/cm^2 [37]. Here, the initial J_{SC} value is found to be 39.17 mA/cm^2 which is somehow lower than the values found in the literature. This is explained by the absence of Ag reflector and MgF_2 as the second anti-reflective coating, and because the as-prepared cell is bifacial. However, it allows

a good transparency of the TPC solar cell studied and could be also improved by different mechanisms, but light soaking in this thesis.

Clearly, the application of normal heat-assisted light soaking on the TPC solar cell increases the *J*sc data up to 39.75 mA/cm^2 compared to 39.6 mA/cm^2 after low-temperature light soaking (360 s, 30 °C). Notwithstanding the confirmed advantageous effect of direct light soaking treatment, a decrease of the *J*sc under heat-assisted dark light soaking is observed for a value of 39.13 mA/cm^2. This finding demonstrates that the contribution of light in the curing process of the TPC solar cell is unavoidable to achieve higher J_{SC} and a good transparency. The results are summarized in figure 24.

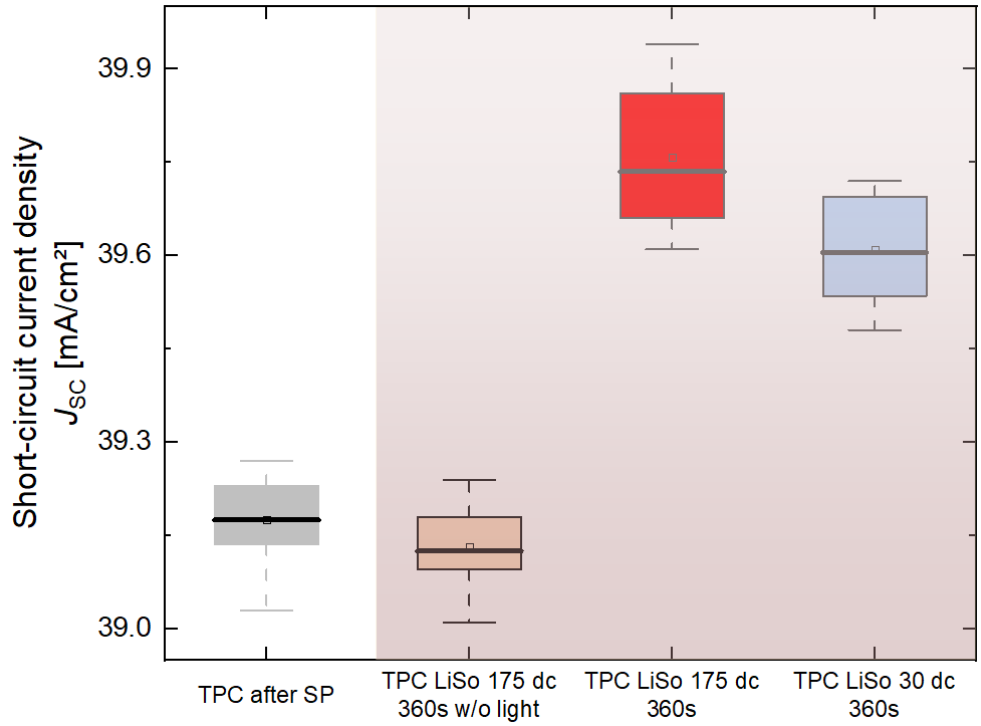

Figure 24: J_{SC} variation for TPC solar cell under different LiSo conditions

The improvements observed for V_{OC}, *FF*, R_S and J_{SC} which mean the improvement of the passivation quality, the conductivity and the transparency subsequently led to an enhancement of the overall power conversion efficiency for the TPC solar cell (Figure 25). The sputter damaged TPC solar cell had an efficiency of 22.05 %. Linked to the highest results recorded at normal light soaking conditions, the best efficiency of 23.4 % is achieved thus for heat-assisted light soaking on the TPC solar cell prepared for this experiment. With low-

temperature light soaking, an efficiency of 22.72 % is accomplished versus 22.22 % under heat-assisted dark light soaking.

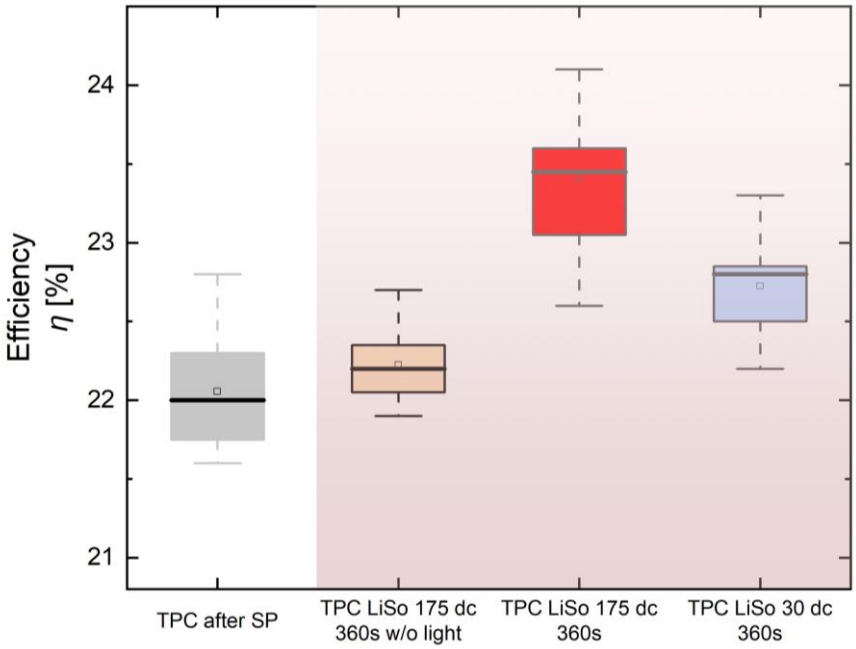

Figure 25: Efficiency variation for TPC solar cell under different LiSo conditions

Since low-temperature light soaking seems to have a potential to enable a good efficiency links to the three photovoltaic parameters, some experiments were also conducted on consecutive low temperature light soaking to investigate its plausible ability and limitations to cure the sputter damage and further boost the efficiency of the TPC solar cell.

Based on the same architecture of the TPC solar cell studied here, the highest recorded efficiency up-to-date is 23.99 % with an error margin of $\pm$0.29 % achieved by [11].

3.2. Comparative study of SHJ and TPC solar cells

The present investigation was done to compare simultaneously the influence of direct heat-assisted light soaking on the TPC structure used as front side and the SHJ architecture used as rear side of the considered TPC-SHJ solar cell. Two solar cells were prepared for this new purpose. The standard light soaking curing was performed based on the respective requirements for each structure (360 s at 175 ℃ with light for TPC and 90 s at 175 ℃ with light for SHJ). Accordingly, the *J-V* data of each cell after ITO deposition and metallization are initially recorded before any curing process.

Compared to SHJ, the TPC structure is more affected by the sputter damage resulting in a lowest open-circuit voltage after ITO deposition (Before LiSo). This means that the sputter damage strongly influences the front side of the solar cell. After standard light soaking, the passivation quality of both SHJ and TPC are greatly recovered (Figure 26). The implied iV_{OC} after light soaking measured for TPC solar is 739.5 mV.

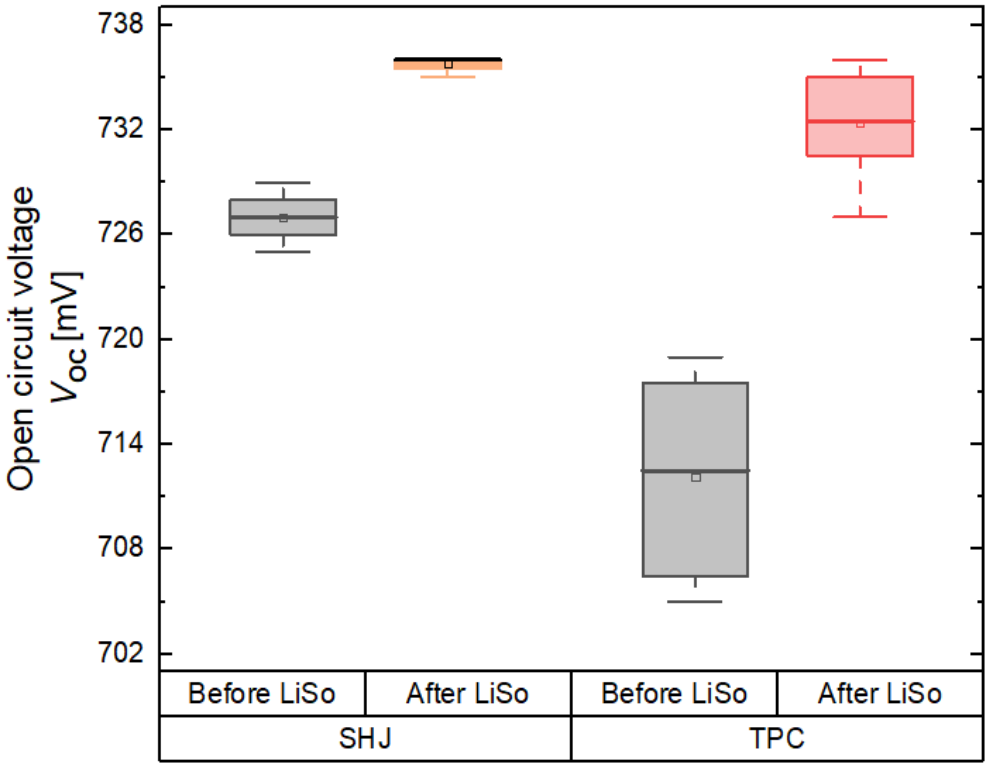

Figure 26: Comparison of the V_{OC} variation for TPC and SHJ after LiSo

For the conductivity evaluation (Figure 27), results show on these new TPC and SHJ solar cells that an achievement of a fill factor of 82.25 % and a series resistance of R_s = 0.641 Ω cm^2 are remarkably possible for SHJ. In the case of the TPC solar cell, a fill factor and a series resistance of 77.42 % and 1.305 Ω cm^2 respectively were recorded. After LiSo, an interesting fill factor of 79.3 % and series resistance of R_s = 1.09 Ω cm^2 are obtained which confirms the previous results and demonstrates the potential of light soaking to improve the electrical properties of the TPC solar cell.

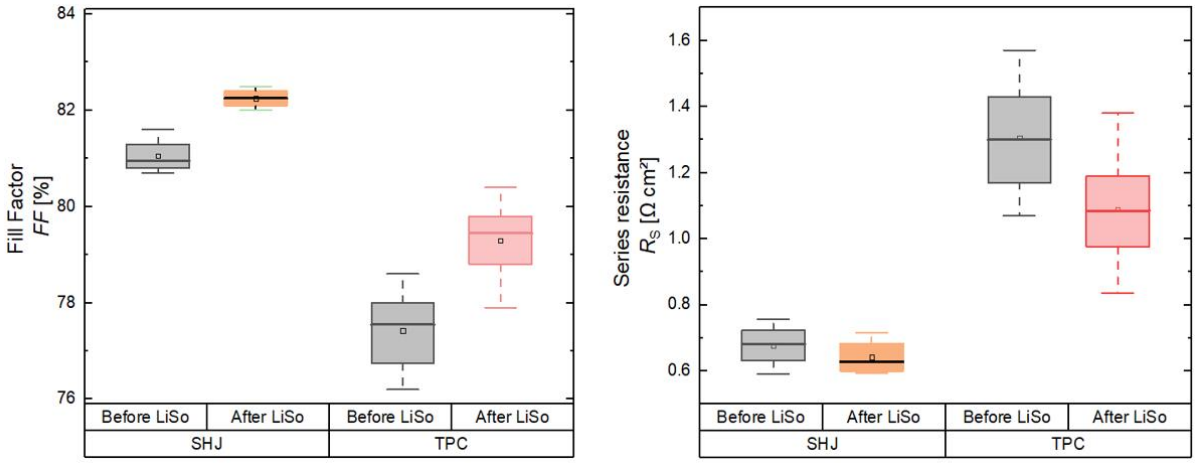

Figure 27: Comparison of (left) *FF* and (right) R_S of SHJ and TPC after LiSo

With its double-layer transparent passivating contact surface, the TPC front side is more transparent than the SHJ rear side. This is better explained by the highest J_{SC} value of 40.27 mA/cm^2 achieved by the considered TPC solar cell compared to the SHJ cell (final J_{SC} = 40.07 mA/cm^2). The results of the comparison of J_{SC} variation for SHJ and TPC solar cells are presented in Figure 28.

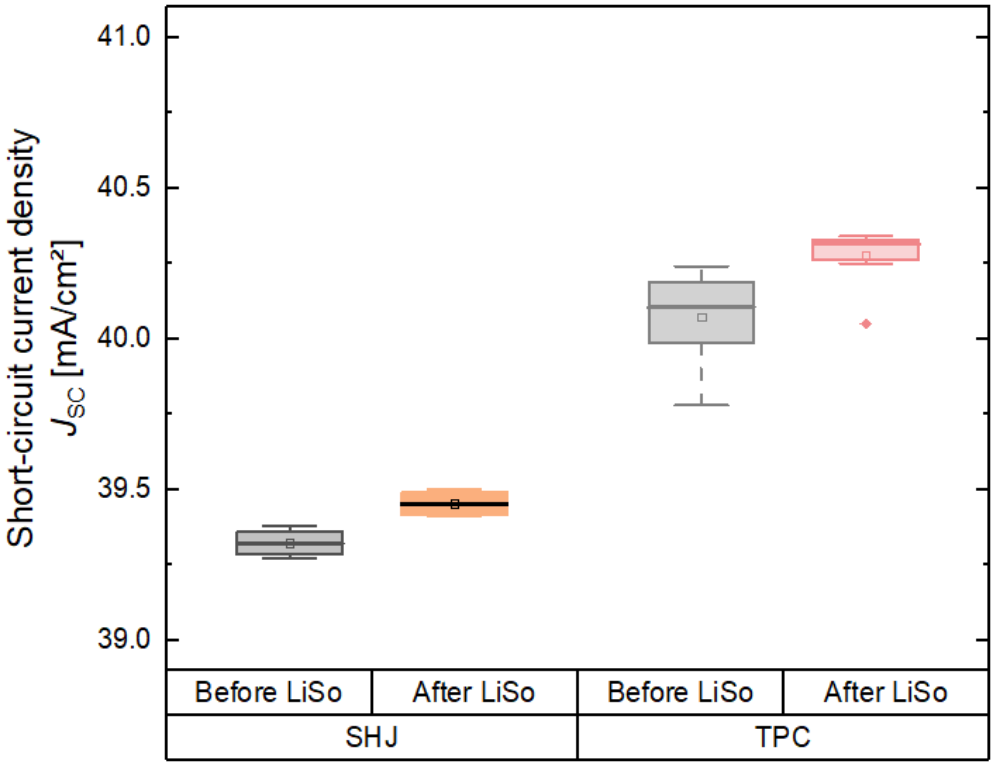

Figure 28: Comparison of J_{SC} variation for SHJ and TPC after LiSo

The power conversion efficiency of the two cells were also compared (Figure 29). Before light soaking curing, the efficiency of TPC and SHJ were 22.08 % and 23.17 %, respectively. After light soaking, an efficiency gain of +1.82% is observed for SHJ and 1.3% for TPC resulting in the final efficiencies of 23.9% and 23.4%, respectively.

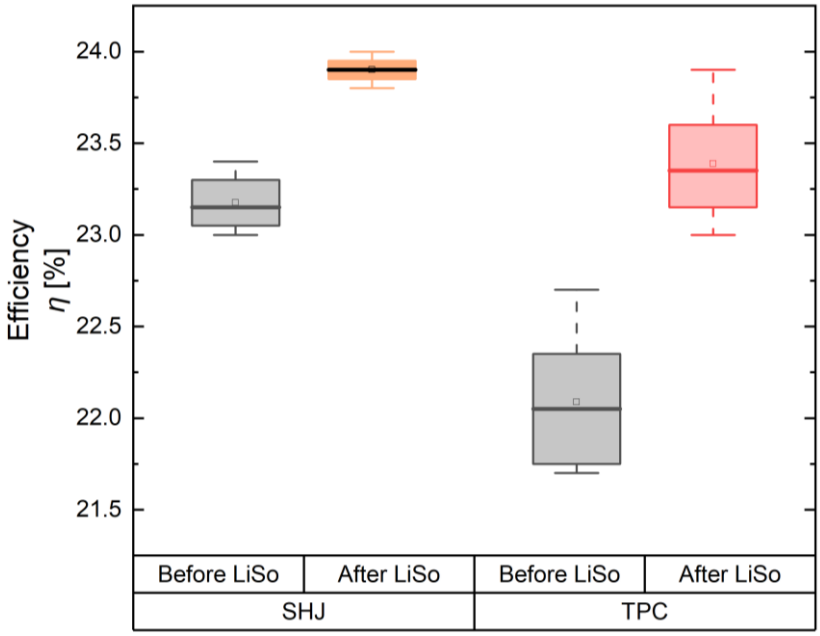

Figure 29: Comparison of efficiency variation for SHJ and TPC after LiSo

The analysis of direct light curing on TPC solar cells and the comparison with SHJ gives the main conclusions that, (i) standard conditions are required for both cells to cure the sputter damage and further enhance the efficiency (ii) the sputter damage is more important on the front side of the TPC-SHJ solar cell and (iii) interesting achievements are made by the TPC with the three photovoltaic parameters resulting in a good transparency, passivation and conductivity, and thus a recorded efficiency of 23.4 %. The different values are summarized in the table 3.

Table 3: Performance achieved by TPC and SHJ in this study.

Cells	η[%]	V_{OC}[mV]	J_{SC}[mA/cm^2]	FF[%]	R_S [Ω cm^2]
TPC	23.4	736.33	39.75	80	1.146
SHJ	23.9	737	39.42	82.2	0.641

3.3. Low temperature light soaking investigation on TPC solar cells

In this section, the low-temperature light soaking conditions to cure the sputter damage and improve the efficiency of the TPC solar cells is thoroughly studied. The study aims at demonstrating the potential and limitations of low-temperature light soaking in solving the passivation loss by applying consecutively this process on the TPC solar cells. As done previously, the experiments were also performed on TPC symmetric samples to monitor the change in implied open-circuit voltage and charge carrier lifetime at the same time.

The application of consecutive low-temperature (low-T) light soaking on the TPC solar cells gradually increases the open-circuit voltage (Figure 30).

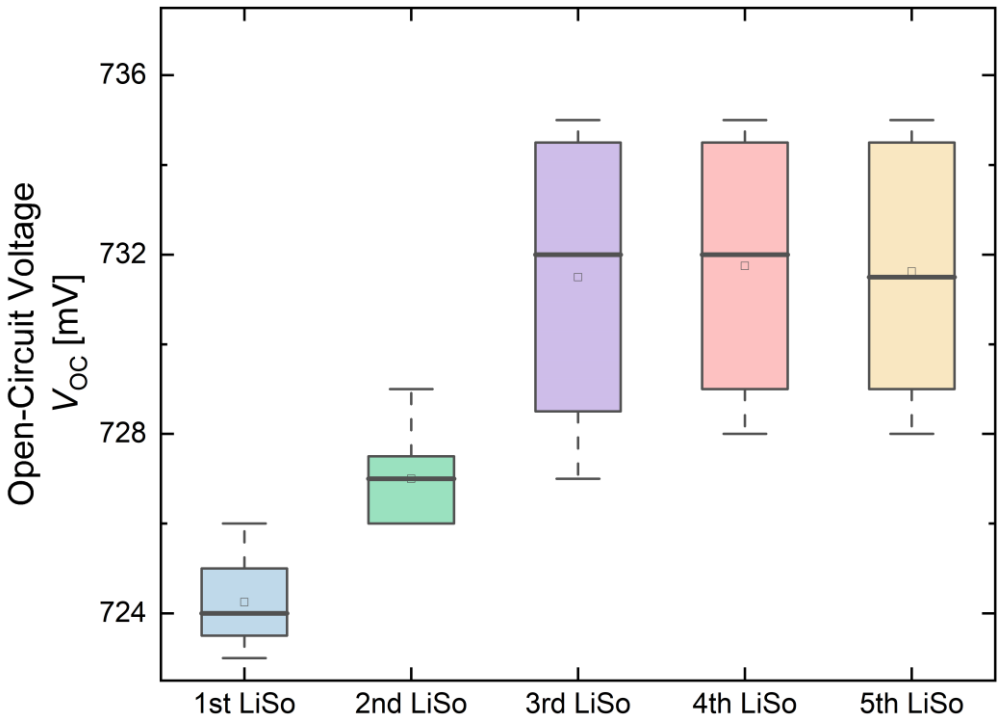

Figure 30: V_{OC} variation of TPC under consecutive low-temperature LiSo

After the first curing, the Voc was 724.25 mV. The second and third curing processes lead to an improvement of 2.5 mV and 4.5 mV respectively which strongly reduces the V_{OC} loss. From the third curing to the 4th low-T light soaking, the passivation quality is slowly recovered. However, after a fifth-time low-T, a decrease of the V_{OC} is observed. The potential of low-T light soaking to recover the passivation quality is thus limited and the process cannot fully cure the sputter damage.

The potential and limitations of low-T light soaking were also tested on the conductivity parameters. As presented in figure 31, the highest fill factor (79.71 %) and lowest series resistance (1.109 Ω cm^2) are achieved after four consecutive low-T light soaking processes.

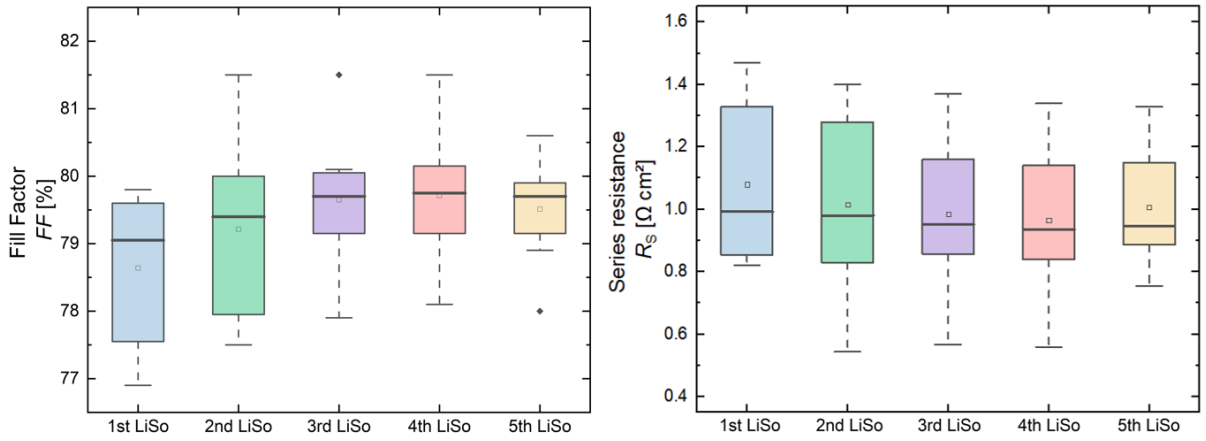

Figure 31: *FF* and R_S variation of TPC under consecutive low-temperature LiSo

A good conductivity is therefore possible with this light curing condition. For the transparency, highest J_{SC} (39.29 mA/cm^2) was reached after five low-T light curing (figure 32) and lowest J_{SC} after third curing steps (39.19 mA/cm^2) which may constitute a limitation and trade-off with the passivation and conductivity parameters.

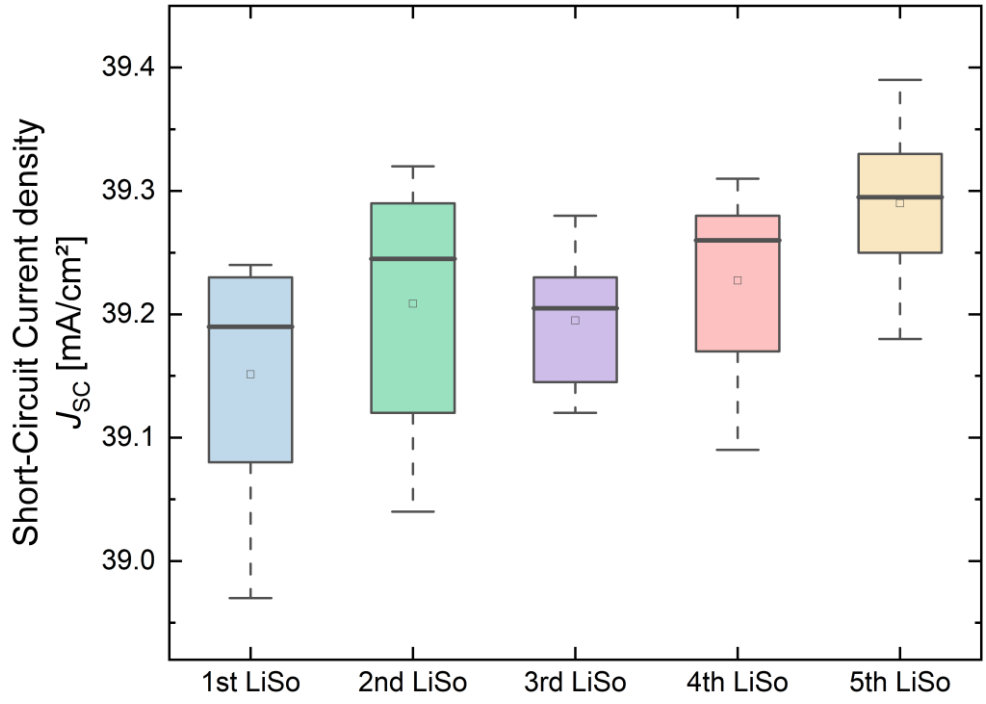

Figure 32: J_{SC} variation of TPC under consecutive low-temperature LiSo

The trend in efficiency gain during the overall process is corelated to the V_{OC} and FF gains. The maximum efficiency achieved is 22.88 % after four consecutive low-T light soaking curing (Figure 33). Compared to direct heat-assisted light soaking, the efficiency gain is low (here +0.58 %; +1.35 % for standard conditions). The conclusion is that the potential of low-temperature light soaking to improve the efficiency of the TPC solar cell is restricted even after some improvements of the passivation quality.

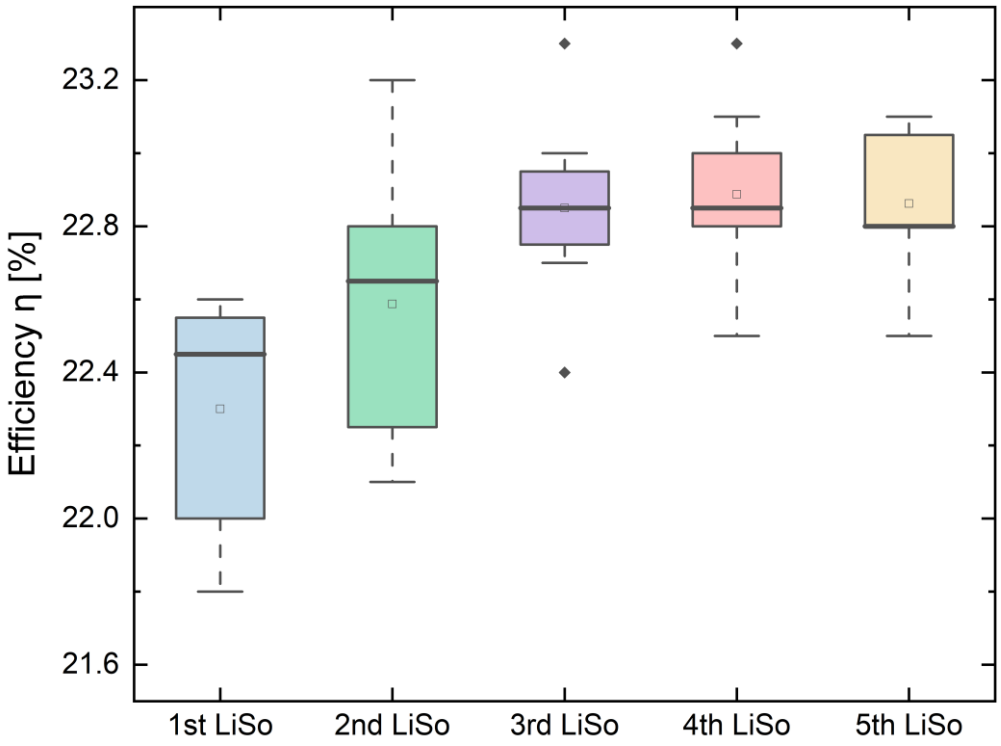

Figure 33: Efficiency variation of TPC under consecutive low-temperature LiSo

To control the V_{OC} loss, the experiments were also conducted on the TPC symmetric samples by QSSPC measurements of effective minority carrier lifetime τ and iV_{OC}. The results were compared with the ones obtained with SHJ symmetric samples.

Table 4: Effective minority carrier lifetime of TPC and SHJ after low-T LiSo.

	Lifetime τ (ms)				
Cells	**1st liso**	**2nd liso**	**3rd liso**	**4th liso**	**5th liso**
TPC	1.209	1.265	1.276	1.294	1.255
SHJ	1.324	1.557	1.674	1.732	1.616

For both cells' structure, the effective carrier lifetime is improved with light soaking (Table 4) up to four consecutive treatments. In the case of heat-assisted light soaking, the improvement was also observed during the experiments. Due to the important effect of sputter damage on front side, the lifetime of charge carriers for TPC is lower compared to SHJ. The consecutive low-temperature light soaking has thus the potential to increase the lifetime of the solar cell.

The implied-open circuit voltage is calculated from the effective minority carrier lifetime as described in chapter 2.

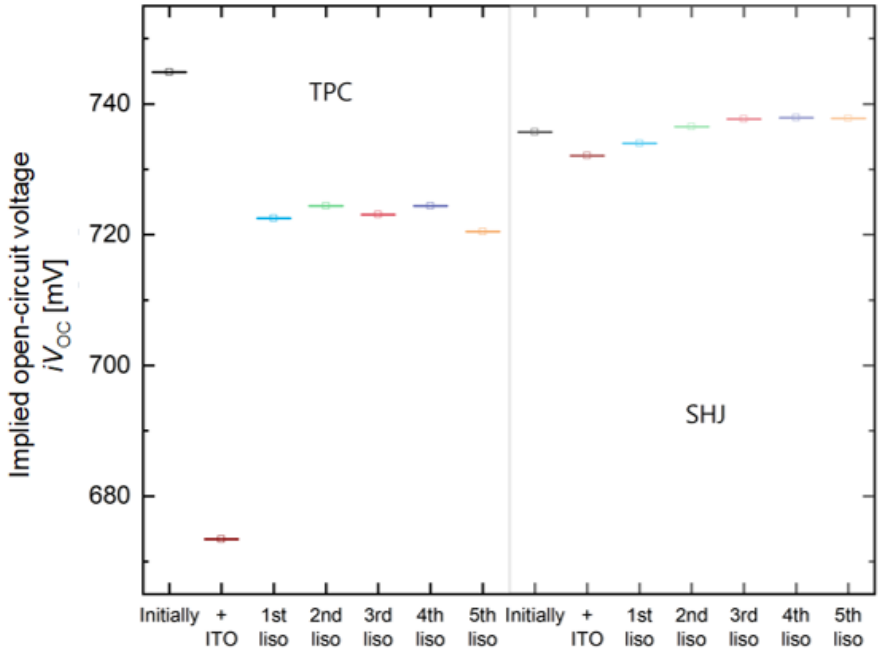

Figure 34: Implied-open circuit voltage variation of TPC and SHJ after low-T LiSo

The process has the potential to recover the passivation (Figure 34) and, as observed on the TPC solar cell with the V_{OC} measurements, the iV_{OC} is subject to some improvements, reaching 724.4 mV as highest iV_{OC} obtained. Since the rear side SHJ is less affected by sputter damage, the low-T light soaking curing processes fully recover the passivation loss in the rear structure.

4. Effect on the electrical properties of nc-SiC:H(n)

The conductivity of nc-SiC:H(n) and the contact resistivity at the Ag/ITO interface were investigated through 2-point and TLM measurements, respectively. During the previous *J-V* measurements for TPC solar cells under direct light soaking, the fill factor (and series

resistance) increases(decreases) leading to an improvement of the conductivity. Therefore, the initial conductivity of the nc-SiC:H(n) layer on glass is measured as a reference value.

As plotted in the bar diagram of figure 35, before ITO deposition and any light curing, the conductivity σ of SiC only is around 8.4×10^{-2} S/cm. For the light curing test, the direct heat-assisted light soaking is used for 360s curing at 175 ℃. The conductivity measured after light soaking is 9.04×10^{-2} S/cm which results in a slight improvement of the conductivity from the reference value. This confirms that the LiSo process can reduce the R_S and then improve the *FF* at the cell level as measured in the previous sections.

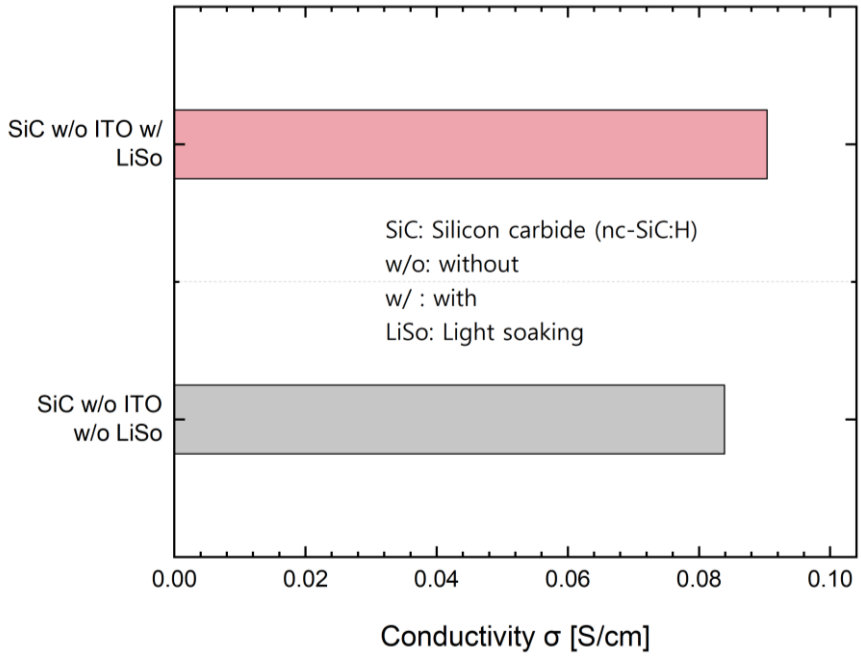

Figure 35: Conductivity of nc-SiC:H(n) before and after LiSo

In the next investigation, five samples are prepared for conductivity measurements (figure 36) and analysis of the effect of light soaking on the prepared layers.

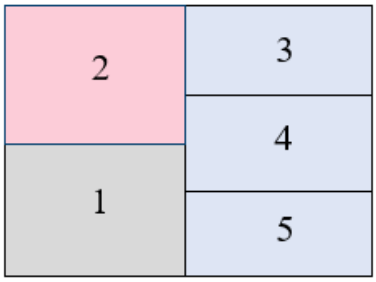

Figure 36: Samples prepared for conductivity measurements

(1) the reference sample made of SiC layer only (2) SiC after heat-assisted light soaking (3) SiC with an ITO layer etched away (4) SiC with the ITO layer etched away before heat-assisted light soaking and (5) SiC with the ITO layer etched away after heat-assisted light soaking.

The etching process of ITO is done during 18 min with a solution of hydrochloric acid (HCl) at 33 % of concentration. This process is performed to remove the ITO layer due to its high conductivity compared to the order of conductivity of SiC. The results are recorded in figure 37.

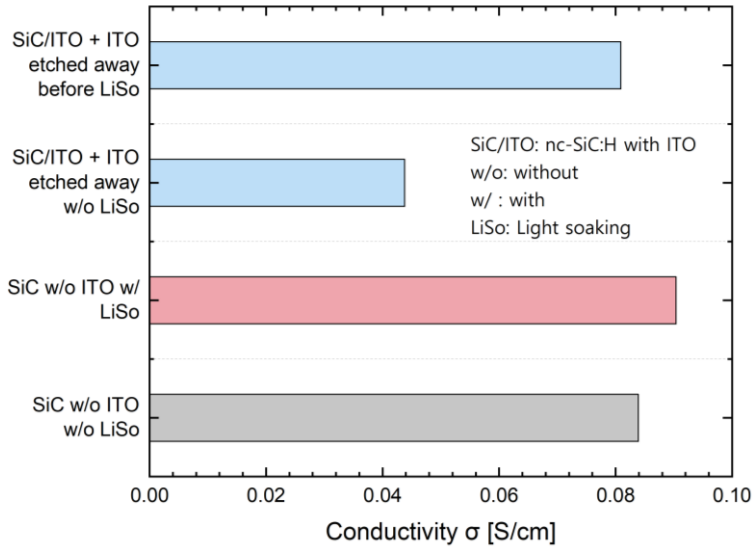

Figure 37: Conductivity variation for different SiC samples

With the etching process of the ITO layer on SiC samples, the conductivity is globally reduced which also means a decrease of the fill factor and a possible increase of the series resistance. The conductivity of the SiC sample with ITO etched away before LiSo process (8.09×10^{-2} S/cm) is quite close to the conductivity of the reference SiC sample. The difference is recorded to be 0.3 S/cm. This result demonstrates the potential of light soaking to recover the conductivity loss. When ITO is etched away after the light curing process, the conductivity decreases significantly. This may be due to the damage caused by the deposition of ITO in addition to the side effect of the etching process. Better results can be obtained by optimizing the etching process (rate of the process, solution used or concentration) or using more accurate methods.

The contact resistivity at the interface between silver and the ITO layer is also measured via the transmission line method. For the three light soaking investigated in this study (low-T,

heat-assisted dark curing, heat-assisted light curing), the contact resistivity for TPC solar cells is measured. The lower the resistive losses the higher the conductivity. The TLM measurement generates a R(d) curve shown in figure 38 (left). This curve is linearly fitted (right) to find the contact resistivity and transfer length through the intercept and slope of the curve.

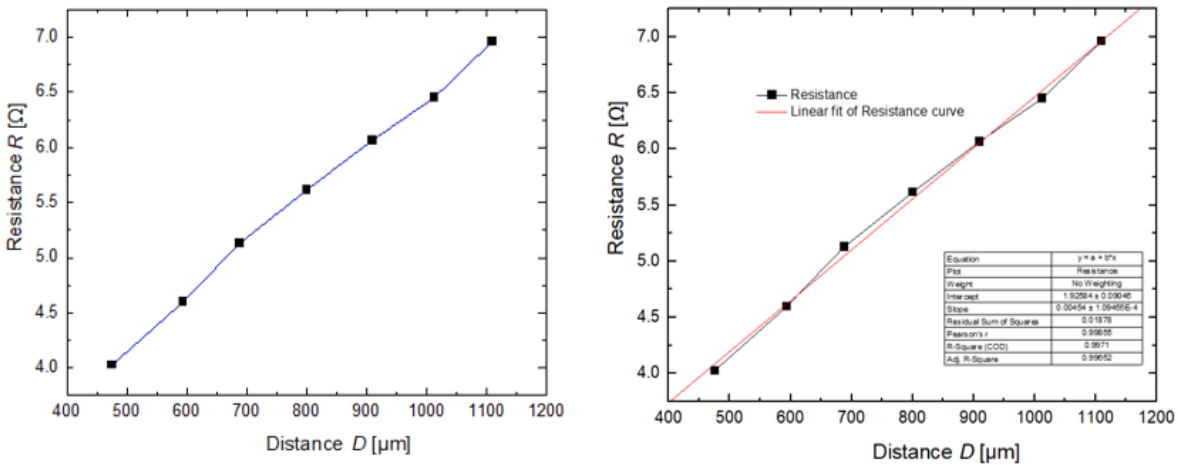

Figure 38: R(d) and linear fit of R(d) curves from TLM

The low contact resistivity of ρ_c= 15.2 mΩ.cm^2 is achieved after heat-assisted light soaking (Figure 39). For SHJ under normal light soaking (90 s, 175 ℃), the contact resistivity measured during the experiment was 9.81 mΩ.cm^2 which is lower than the TPC solar cell. The resistivity of Ag/ITO is therefore more important in TPC and should be reduced for a better conductivity.

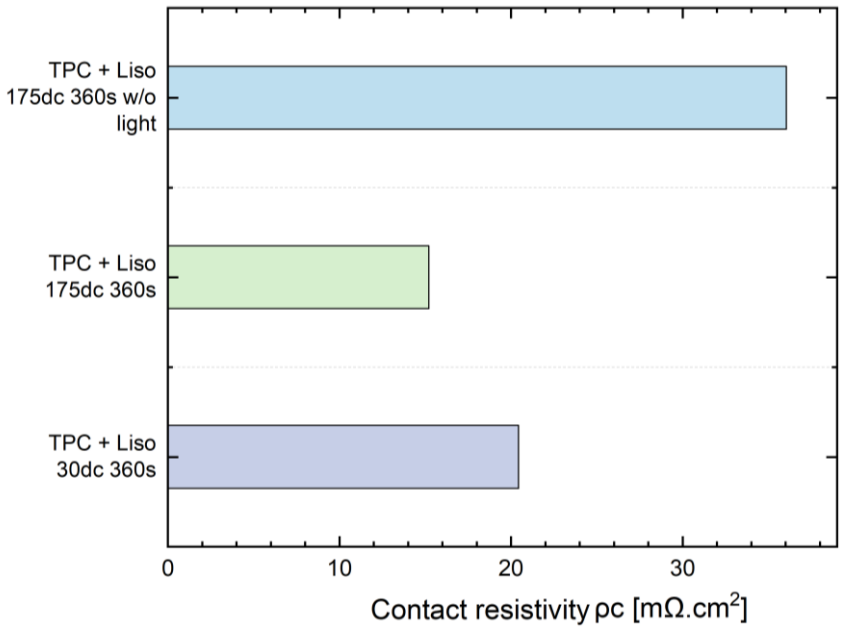

Figure 39: Contact resistivity variation under different LiSo

5. Effect on the structural properties of SiC-based samples

The chemical composition of the nc-SiC as well as the absorbance of the material is evaluated through FTIR spectroscopy. In this section, low-temperature light soaking and heat-assisted light soaking are applied on the SiC samples to investigate the effect of these curing of the absorbance of the material. After measurement, the absorbance of c-Si substrate is subtracted from the results obtained via asymmetric least square smoothing baseline analysis.

The FTIR spectra before the direct light soaking treatments of the c-Si(n) double side polished wafer show the stretching bonds of SiC around 800 cm^{-1}. The analysis of the spectra also shows some absorption bands around 2100 cm^{-1} due to the presence of Si-H_2 (poly-hydrides) which may come from the plasma.

After both low-T and heat-assisted light soaking treatments, the absorbance of the c-Si(n) wafer in the range of wavenumber considered is almost unchanged (figure 41).

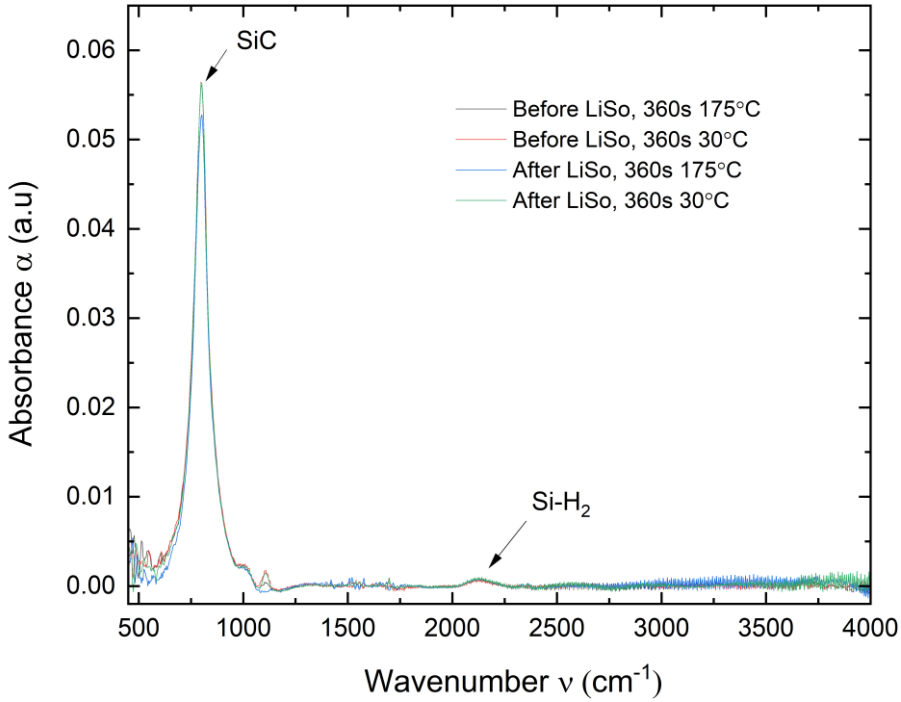

Figure 40: FTIR measurement of c-Si(n) wafer

It is concluded that the direct light soaking has no significant effect on the absorbance of the c-Si(n) under IR. Notwithstanding, the FTIR spectroscopy is not the more accurate material characterization for the c-Si wafer. Some more precise and well-developed experimental methods such as Raman could be used for better investigations.

CONCLUSION AND PERSPECTIVES

The light soaking process without pre-annealing treatment and its potential to solve the degradation of the passivation quality due to ITO sputtering in transparent passivating contact solar cells was examined. The present study aimed at curing the sputter damage and provides a better understanding of the light curing to enable high efficiency TPC-SHJ solar cells. A comparison between the sputter damage on the front TPC structure and the rear SHJ structure demonstrated that the TPC structure is mostly affected by the sputter damage. Heat-assisted light soaking performed at 175 ℃ during 360 s was found to be the effective setting to reduce the V_{OC} loss in TPC solar cells, which can also improve the *FF* and J_{SC}. In this study, a V_{OC} of 736mV was achieved after light soaking resulting in a final V_{OC} loss of only 6mV (initial V_{OC} loss = 28 mV). The passivation was strongly recovered, and the improvements made on the cell enable *FF* = 80%, R_S = 1.146 Ω cm^2, J_{SC} = 39.75 mA/cm^2 for an overall PCE of 23.4%. Alternative light curing processes were studied. The low-temperature light soaking and heat-assisted dark curing show a minimal improvement of the passivation quality, demonstrating the unavoidable need for both light source and thermal effects.

Despite the important achievements made, the present study has some limitations. The conductivity of only Ag/ITO interface was considered due to some challenges in successfully measuring the resistivity between the silver contact and the TPC n-type stack. Previous studies have demonstrated that the contact resistivity of Ag/ITO is negligible in comparison to the Ag/TPC stack. Therefore, to draw final conclusions on the effect of direct light soaking curing on the electrical properties of nc-SiC:H(n), the resistivity of Ag/n-type stack should also be measured and combined with the results obtained here. Moreover, the electrical and material characterizations under direct light soaking of respectively nc-SiC:H(n) and c-Si(n) wafer could be more accurately investigated via a four-point conductivity measurement and some material methods such us Raman, Secondary Mass Ion Spectroscopy (SIMS) and Electrochemical Capacitance Voltage (ECV). Due to the short-period of time, these characterization methods were not performed in addition to an activation energy calculation of the light soaking planned at low and high temperatures. These limitations constitute some perspectives for future studies. The present study contributes to the definition of a pathway towards the achievement of highly efficient silicon-based solar cells with transparent passivating contact surfaces.

BIBLIOGRAPHIC REFERENCES

[1] H. Ritchie, M. Roser, and P. Rosado, "Our World In Data", *CO2 and Greenhouse Gas Emissions*, 2020, https://ourworldindata.org/co2-and-greenhouse-gas-emissions (accessed Apr. 06, 2023).

[2] IEA - International Energy Agency, "Electricity production," *Share of electricity produced from solar from 1985 to 2022. Retrieved by Our World Our Data*, 2023, https://www.energyinst.org/statistical-review/ (accessed Jun. 11, 2023).

[3] IEA - International Energy Agency, "Electricity Information: Overview", 2021. https://www.iea.org/reports/electricity-information-overview, License: CC BY 4.0 (accessed May 05, 2023).

[4] SolarPower Europe, "Global Market Outlook for Solar Power 2022-2026," *Cumulative installed solar PV capacity worldwide from 2000 to 2021 (in megawatts) [Graph]. In Statista. Retrieved August 07, 2023, from https://www.statista.com/statistics/280220/global-cumulative-installed-solar-pv-capacity/*, (2022).

[5] A. Louwen, W. Van Sark, R. Schropp, and A. Faaij, "A cost roadmap for silicon heterojunction solar cells," *Solar Energy Materials and Solar Cells*, vol. 147, pp. 295–314, 2016.

[6] NREL - National Renewable Energy Laboratory, "Best Research Cell Efficiency," *U.S. Department of Energy*, 2022. https://www.nrel.gov/pv/cell-efficiency.html

[7] J. Melskens, B. W. H. Van De Loo, B. Macco, L. E. Black, S. Smit, and W. M. M. Kessels, "Passivating Contacts for Crystalline Silicon Solar Cells: From Concepts and Materials to Prospects," *IEEE Journal of Photovoltaics*, vol. 8, no. 2, pp. 373–388, 2018.

[8] K. Ding, M. Pomaska, A. Singh, F. Lentz, F. Finger, and U. Rau, "Mechanism for crystalline Si surface passivation by the combination of SiO_2 tunnel oxide and μc-SiC:H thin film," *Physica Status Solidi (RRL) - Rapid Research Letters*, vol. 10, no. 3, pp. 233–236, 2015.

[9] M. Köhler *et al.*, "Optimization of Transparent Passivating Contact for Crystalline Silicon Solar Cells," vol. 10, no. 1, pp. 46–53, 2020.

[10] M. Köhler *et al.*, "Development of a Transparent Passivated Contact as a Front Side Contact for Silicon Heterojunction Solar Cells," *In IEEE 7th World Conference on Photovoltaic Energy Conversion (WCPEC)*, pp. 3468–3472, 2018.

[11] M. Köhler *et al.*, "A silicon carbide-based highly transparent passivating contact for crystalline silicon solar cells approaching efficiencies of 24%," *Nature Energy*, vol. 6, no. 5, pp. 529–537, 2021.

[12] A. Reinders, P. Verlinden, W. Van Sark, and A. Freundlich, "Photovoltaic solar energy: From fundamentals to Energy," John Wiley & Sons Ltd., 2017.

[13] J. A. Luceño-Sánchez, A. M. Díez-Pascual, and R. P. Capilla, "Materials for photovoltaics: State of art and recent developments," *International Journal of Molecular Sciences*, vol. 20, no. 4, 2019.

[14] S. N. Karthick, K. V. Hemalatha, S. K. Balasingam, F. Manik Clinton, S. Akshaya, and H. J. Kim, "Dye-sensitized solar cells: History, components, configuration, and working principle," Interfacial Engineering in Functional Materials for Dye-Sensitized Solar Cells, no. December, pp. 1–16, 2019.

[15] K. Mertens, "Photovoltaics: Fundamentals, Technology and Practice"*, John Wiley & Sons Ltd.,* no. May, pp. 1-368*,2018*.

[16] A. R. Zanatta, "The Shockley–Queisser limit and the conversion efficiency of silicon-based solar cells," *Results in Optics*, vol. 9, no. October, p. 100320, 2022.

[17] A. Blakers, N. Zin, K. R. McIntosh, and K. Fong, "High efficiency silicon solar cells," *Energy Procedia*, vol. 33, pp. 1–10, 2013.

[18] M. A. Green, J. Zhao, A. Wang, P. J. Reece., and M. Gal, "Efficient Silicon Light-emitting diodes," *Nature*, vol. 421, no. August, pp. 805–808, 2001.

[19] David Herrmann, "Characterization of Metallization-Induced Recombination Losses of Screen-Printed Silicon Solar Cells," Dissertation, Albert-Ludwigs-Universität Freiburg, Germany, 2021.

[20] J. Zhao, "Recent advances of high-efficiency single crystalline silicon solar cells in processing technologies and substrate materials," *Solar Energy Materials and Solar Cells*, vol. 82, no. 1–2, pp. 53–64, 2004.

[21] Prof. Dr. U. Rau, “Photovoltaics II Characterisation and Simulation of Solar Cells-Chapter I,” Lecture material, Abdou Moumouni University, Niger, 2023.

[22] M. S. Bazilchuk, “Improved Induced Diode Photodetectors by Increased Fixed Charge in PECVD Amorphous Silicon Nitride,” no. June, 2014.

[23] Y. Liu *et al.*, “High-Efficiency Silicon Heterojunction Solar Cells: Materials, Devices and Applications,” *Materials Science and Engineering: R: Reports*, vol. 142, no. May, 2020.

[24] A. Augusto, S. Y. Herasimenka, R. R. King, S. G. Bowden, and C. Honsberg, “Analysis of the recombination mechanisms of a silicon solar cell with low bandgap-voltage offset,” *Journal of Applied Physics*, vol. 121, no. 20, 2017.

[25] A. Cuevas, “The recombination parameter J_0,” *Energy Procedia*, vol. 55, pp. 53–62, 2014.

[26] D. A. R. Barkhouse, O. Gunawan, T. Gokmen, T. K. Todorov, and D. B. Mitzi, “Yield predictions for photovoltaic power plants:empirical validation,recent advances and remaining uncertainties,” *Progress in Photovoltaics : Research and Applications*, vol. 20, no. 1, pp. 6–11, 2015.

[27] A. Khanna, T. Mueller, R. A. Stangl, B. Hoex, P. K. Basu, and A. G. Aberle, “A Fill Factor Loss Analysis Method for Silicon Wafer Solar Cells,” *IEEE Journal of Photovoltaics*, vol. 3, no. 4, pp. 1170–1177, 2013.

[28] S. Siebentritt, “Photovoltaics - The Shockley-Queisser limit,” Laboratory for Photovoltaivs, Department of Physics and Materials Science, University of Luxxembourg, 2021.

[29] D. Abou-ras, T. Kirchartz and U. Rau, “Advanced Characterization Techniques for Thin Film Solar Cells, ” *Wiley VCH*, 2011.

[30] O. D. Miller, E. Yablonovitch, and S. R. Kurtz, “Strong internal and external luminescence as solar cells approach the Shockley-Queisser limit,” *IEEE Journal of Photovoltaics*, vol. 2, no. 3, pp. 303–311, 2012.

[31] B. Ehrler, E. Alarcón-Lladó, S. W. Tabernig, T. Veeken, E. C. Garnett, and A. Polman, “Photovoltaics reaching for the shockley-queisser limit,” *ACS Energy Letters*, vol. 5, no.

9, pp. 3029–3033, 2020.

[32] S. Rühle, “Tabulated values of the Shockley-Queisser limit for single junction solar cells,” *Solar Energy*, vol. 130, pp. 139–147, 2016.

[33] ISE-Frauhonfer Institute for Solar Energy Systems, “Photovoltaics Report,” Friedburg, no. February, 2023.

[34] S. Tsuda *et al.*, “a-Si technologies for high efficiency solar cells,” *Journal of Non-Crystalline Solids*, vol. 164–166, no. Part 2, pp. 679–684, 1993.

[35] G. Cook, L. Billman and R. Adcock,“Photovoltaic Fundamentals”, *National Renewable Energy Laboratory, U.S. Department of Energy*,1995.

[36] H. Park *et al.*, “Front and Back TCO Research Review of a-Si/c-Si Heterojunction with Intrinsic Thin Layer (HIT) Solar Cell,” *Transactions on Electrical and Electronic Materials*, vol. 19, no. 3, pp. 165–172, 2018.

[37] Z. Fiedler, “Material and process development to optimize the short-circuit current density of nc-SiC:H(n) based TPC solar cells”, Master thesis, Ruhr-Universität Bochum, Germany, 2022.

[38] M. Köhler et *al.*, “Supplementary information :A silicon carbide-based highly transparent passivating contact for crystalline silicon solar cells approaching efficiencies of 24 %”, Nature Energy, vol. 6, pp. 529–537, 2021.

[39] E. Kobayashi *et al.*, “Light-induced performance increase of silicon heterojunction solar cells,” *Applied Physics Letters*, vol. 109, pp. 1–6, 2016.

[40] K. Qiu *et al.*, “A comprehensive study of the light soaking effect in ZnS/p-Si heterojunction solar cells,” *Solar Energy*, *Elsevier*, vol. 225, no. August, pp. 961–968, 2021.

[41] C. R. Wronski, “Chapter 10 : The Staebler-Wronski Effect,” *Semiconductors and Semimetals*, vol. 21, no. Part C, pp. 347–374, 1984.

[42] S. Bao *et al.*, “The rapidly reversible processes of activation and deactivation in amorphous silicon heterojunction solar cell under extensive light soaking,” *Journal of Materials Scence: Materials in Electronics*, vol. 32, no. February, pp. 4045–4052, 2021.

[43] M. Gostein and L. Dunn, “Light Soaking Effects on PV Modules: Overview and

Literature Review," In 37th IEEE *Photovoltaic Specialists Conference (PVSC)*, Seattle, Washington, no. June, pp. 1–25, 2011.

[44] H. Fujiwara, "Spectroscopic Ellipsometry: Principles and Applications", *John Wiley & Sons*, National Institute of Advanced Industrial Science and Technology, Japan, 2007.

[45] MD G. Uddin, "Development of Simplified In Situ Processing Routes for Rear-Side Patterning of Silicon Heterojunction Interdigitated Back Contact (SHJ-IBC) Solar Cells", Master Thesis, University of Eastern Finland, Finland, 2019.

[46] Prof. Dr. U. Rau, "Characterization and simulation of solar cells - Electroluminescence Overview", Lecture material, Abdou Moumouni University, Niger, 2023.

[47] T. Rudolph, "Application of Intensive Light Soaking on Silicon Heterojunction Solar Cells and Modules", Master Thesis, RWTH Aachen University, Germany, 2022.

[48] A. H. T. Le *et al.*, "Damage to passivation contact in silicon heterojunction solar cells by ITO sputtering under various plasma excitation modes," *Solar Energy Materials and Solar Cells*, vol. 192, no. April, pp. 36–43, 2019.

[49] D. Zhang, A. Tavakoliyaraki, Y. Wu, R. A. C. M. M. Van Swaaij, and M. Zeman, "Influence of ITO deposition and post annealing on HIT solar cell structures", *Energy Procedia*, vol. 8, no. April, pp. 207–213, 2011.

APPENDIX

A Symbols

Symbols	Definitions	Units
FF	Fill Factor	%
iV_{OC}	Implied open-circuit voltage	mV
J_{SC}	Short-circuit current density	mA/cm^2
R_S	Series resistance	Ω cm^2
S_{eff}	Surface recombination velocity	cm/s
T_F	Filament temperature	℃
V_{OC}	Open-circuit voltage	mV
α	Absorbance	-
η	Efficiency	%
ν	Wavenumber	cm^{-1}
ρ_C	Contact resistivity	mΩ.cm^2
τ	Lifetime	ms
σ	Conductivity	S/cm

B Supplementary characterization data

B.1 Light Soaking Spectrum Characterization

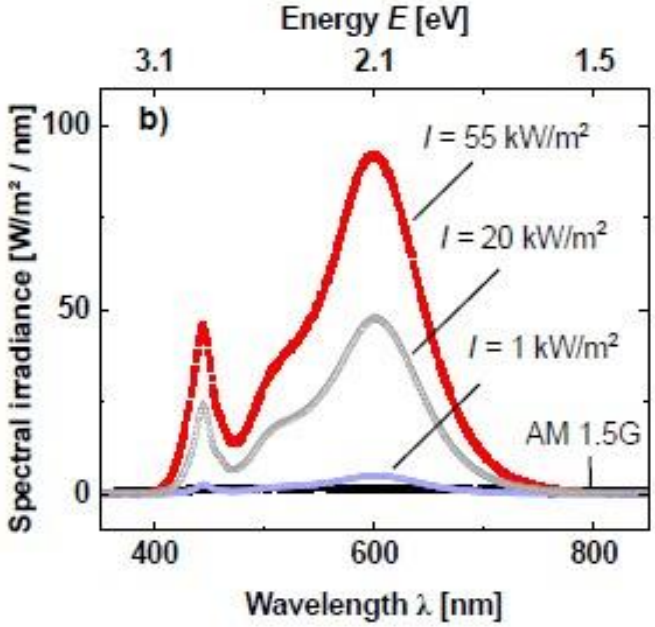

Figure 41: Absolute spectral irradiance under different light intensities. The red curve is the spectrum of light considered in the study. Taken from [47].

B.2 Electroluminescence images of TPC solar cells

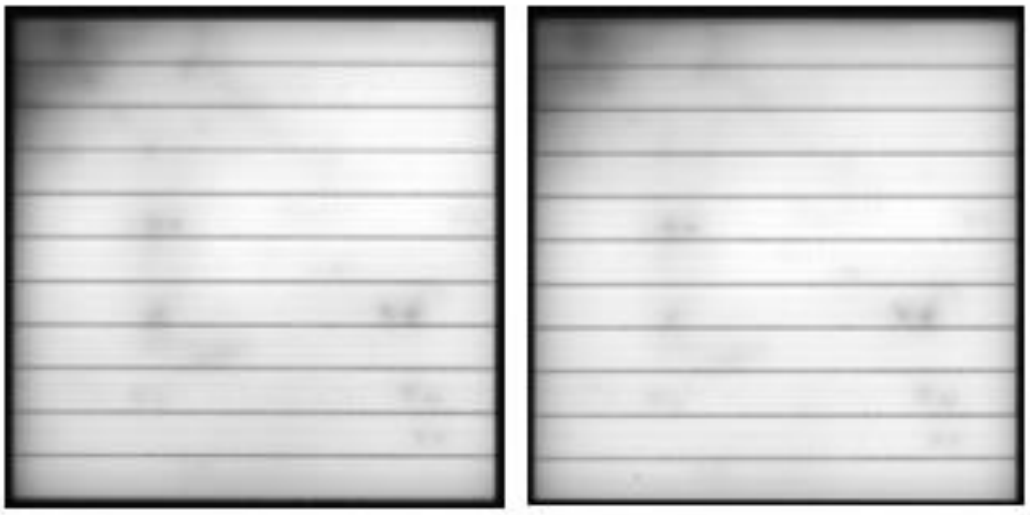

Figure 42: EL images for TPC solar cell (position 1) after low-T LiSo

B.3 FTIR spectra for nc-SiC

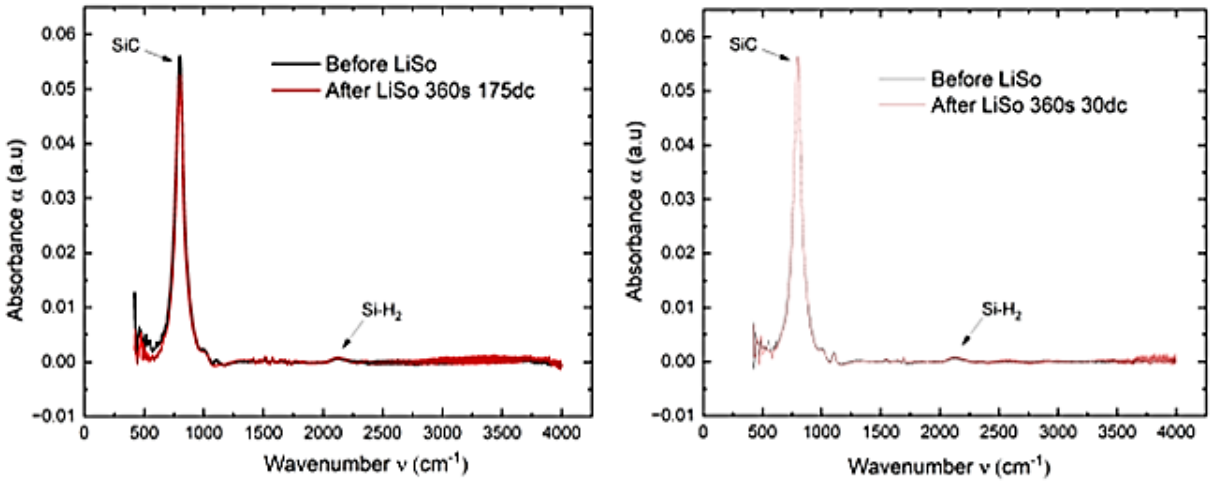

Figure 43: FTIR spectra before and after LiSo